

Consequences of DM/antiDM Oscillations for Asymmetric WIMP Dark Matter

Marco Cirelli^{a,b}, Paolo Panci^{a,c,d,e,f},
Géraldine Servant^{a,b}, Gabrijela Zaharijas^{b,g},

^a *CERN Theory Division, CH-1211 Genève, Switzerland*

^b *Institut de Physique Théorique, CNRS, URA 2306 & CEA/Saclay, F-91191 Gif-sur-Yvette, France*

^c *Dipartimento di Fisica, Università degli Studi dell'Aquila, 67010 Coppito (AQ)*

^d *INFN, Laboratori Nazionali del Gran Sasso, 67010 Assergi (AQ), Italy*

^e *Université Paris 7-Diderot, UFR de Physique, 10, rue A. Domon et L. Duquet, 75205 Paris, France*

^f *CP³-origins & the Danish Institute for Advanced Study DIAS,
University of Southern Denmark, Campusvej 55, DK-5230 Odense M, Denmark*

^g *Institut d'Astrophysique de Paris, UMR 7095-CNRS &
Université Pierre et Marie Curie, boulevard Arago 98bis, 75014, Paris, France.*

Abstract

Assuming the existence of a primordial asymmetry in the dark sector, a scenario usually dubbed Asymmetric Dark Matter (aDM), we study the effect of oscillations between dark matter and its antiparticle on the re-equilibration of the initial asymmetry before freeze-out, which enable efficient annihilations to recouple. We calculate the evolution of the DM relic abundance and show how oscillations re-open the parameter space of aDM models, in particular in the direction of allowing large (WIMP-scale) DM masses. A typical wimp with a mass at the EW scale (~ 100 GeV – 1 TeV) presenting a primordial asymmetry of the same order as the baryon asymmetry naturally gets the correct relic abundance if the DM-number-violating $\Delta(\text{DM}) = 2$ mass term is in the \sim meV range. The re-establishment of annihilations implies that constraints from the accumulation of aDM in astrophysical bodies are evaded. On the other hand, the ordinary bounds from BBN, CMB and indirect detection signals on annihilating DM have to be considered.

1 Introduction

Dark Matter (DM) constitutes a sizable fraction of the current energy density of the Universe, corresponding to $\Omega_{\text{DM}}h^2 = 0.1126 \pm 0.0036$ [1]¹. A leading explanation for DM in the last three decades has been to postulate the existence of a cosmologically stable weakly-interacting massive particle (WIMP), as well-motivated by Standard Model extensions at the electroweak scale. Most of the proposed candidates arising in these frameworks are either their own antiparticles (e.g. the Majorana neutralino in SUSY) or it is assumed that DM particles and anti-particles are produced in equal numbers, in contrast to what happens in the visible sector, i.e. for baryons. The origin of DM in both cases is explained in terms of the standard freeze-out mechanism, by which the annihilations of DM and its anti-particle naturally stop when the expansion of the universe overcomes the strength of their cross section, thus leaving the current DM abundance as the left-over of an incomplete annihilation process. The only crucial parameter setting Ω_{DM} , in this standard framework, is indeed the annihilation cross section.

With the experimental programme to search for WIMPs being close to reaching its culmination point, theorists have increasingly considered deviations with respect to standard paradigm presented above. One route is to assume a different cosmological history [2], or to consider very feebly interacting particles which would have never reached thermal equilibrium [3, 4].

Another possibility is to assume that DM particles were once in thermal equilibrium *with an initial asymmetry* between particles and anti-particles, as originally considered in Technicolor-like constructions [5, 6, 7, 8, 9] or mirror models [10, 11, 12, 13, 14, 15, 16], but also in other contexts [17, 18, 19, 20, 21, 22]. In the latest two years, there has been a revival of interest for this scenario, dubbed Asymmetric Dark Matter (aDM) [23, 24, 25, 26, 27, 28, 29, 30, 31, 32, 33, 34, 35, 36, 37, 38, 39, 40, 41, 42, 43, 44, 45, 46, 47, 48], with the aim in particular of connecting the DM abundance to the abundance of baryons, i.e. to understand the origin of the ratio $\Omega_{\text{B}}/\Omega_{\text{DM}} \sim 1/5$. ($\Omega_{\text{B}}h^2 = 0.0226 \pm 0.00053$ [1]). A common production history for the dark and visible matter, in fact, provides an elegant explanation of why the two densities are so close to each other. This approach, in its simplest realizations, suggests a rather light particle, $\mathcal{O}(5 \text{ GeV})$: this does not match the expected scale of new physics, but part of the community has seen in it intriguing connections with some recent hints of signals in various direct detection experiments [49].² Like for the baryonic abundance, if there is an asymmetry in the dark sector, as soon as annihilations have wiped out the density of (say) antiparticles, the number density of particles remains frozen for lack of targets, and is entirely controlled by the primordial asymmetry rather than by the value of the annihilation cross section. This is why this scenario appears rather constraining on the value of the DM mass.

This conclusion, however, changes in the presence of oscillations between DM and antiDM particles, and it is the purpose of this paper to study this in detail. Such oscillations can indeed replenish the depleted population of ‘targets’. Annihilations, if strong enough,

¹Here $\Omega_{\text{DM}} = \rho_{\text{DM}}/\rho_{\text{c}}$ is defined as usual as the energy density in dark matter with respect to the critical energy density of the Universe $\rho_{\text{c}} = 3H_0^2/8\pi G_N$, where H_0 is the present Hubble parameter. h is its reduced value $h = H_0/100 \text{ km s}^{-1}\text{Mpc}^{-1}$.

²Some works have however shown how the connection between the baryon asymmetry and the DM asymmetry can be preserved even for DM particles with masses in the WIMP (100 GeV – 1 TeV) range e.g. [28].

can then re-couple and deplete further the DM/antiDM abundance. The final DM relic abundance is therefore attained through a more complex history than in the standard case of aDM, and in closer similarity to the freeze-out one. Somehow, the phenomenology associated to oscillations has not been yet studied in detail. The effect of oscillations between DM and $\overline{\text{DM}}$ was mentioned only a few times in the literature [24, 25, 31, 37, 46]. In these works, an oscillation mechanism between particles and antiparticles was considered only at late times. In fact, oscillations were prevented by assumption from occurring too early, when annihilations are still coupled, in order to maintain the simple relation between the DM asymmetry and the baryon asymmetry. We are in contrast interested in the opposite situation where oscillations do play a role and control the final relic abundance. This situation is possible and not unlikely: there is no specific physical reason why oscillations could not start early on, and therefore this situation should not be disregarded. Moreover, it is an instructive setup in the sense that it fills a gap between the standard thermal freeze out prediction (where Ω_{DM} does not depend explicitly on the DM mass but only on the annihilation cross section $\langle\sigma v\rangle$), and the aDM prediction where $\Omega_{\text{DM}}h^2$ does not depend on $\langle\sigma v\rangle$ but only on the primordial DM asymmetry.

Another interesting consequence of adding oscillations on top of aDM concerns the phenomenological bounds. Bounds on the traditional aDM framework have been studied in several works [52]: most constraints follow from possible decays of aDM particles or from the effect of accumulation in stars. If, however, aDM annihilates again at late times, as it does in the scenarios that we are considering, most of such bounds are evaded in a natural way. On the other hand, the revival of annihilations leads to indirect detection signals and subjects our framework to the usual constraints on annihilating DM, as we will discuss below.

The rest of the paper is organized as follows. In Section 2 we briefly review some theory motivations for having DM/antiDM oscillations and we make contact between the phenomenological parameter δm , which enters in the physics of oscillations, and the scales of possible underlying particle physics models. In Sec. 3 we lay down the formalism that we use for treating the system of annihilating and oscillating DM particles, and we illustrate the outcome in a few illustrative cases. We also include in the treatment the elastic scatterings that DM particles have with the primordial plasma and see that these can have an important effect in modifying the evolution. In [50] and [51] a detailed study of the evolution (Boltzmann) equations of the populations of aDM has been performed: our work is a generalization of these results to the case in which DM and $\overline{\text{DM}}$ oscillations also happen. In Sec. 4 we present more systematically the results as a function of the choices of parameters in the system, and individuate the interesting regions of the parameter space. In Sec. 5 we discuss the impact of the current constraints (from cosmology, astrophysics and colliders) on our parameter space. Finally, Sec. 6 summarizes our conclusions.

2 Theory motivations

In this work we assume that the dark matter particle DM is not its antiparticle $\overline{\text{DM}}$ and we assume that there is a primordial asymmetry between the two populations. We will follow a phenomenological approach, in the sense that we are agnostic about the the origin of such primordial asymmetry: we only assume its existence and we study the evolution of the two populations in the presence of oscillations generated by a $\Delta(\text{DM}) = 2$ mass term,

δm . We assume that all operators responsible for the asymmetry are switched off when we start following the evolution, which is reasonable when considering WIMP-scale particles.

The effect of $\Delta(\text{DM}) = 2$ operators is to introduce a mass splitting and mixing between DM and $\overline{\text{DM}}$, which are no longer mass eigenstates. Oscillations will be cosmologically relevant if $\delta m \gtrsim H \sim T^2/m_{Pl}$. Therefore, it is clear that for a too large δm , oscillations will start too early, well before annihilations freeze-out and we recover a standard symmetric DM freeze-out scenario. If on the other hand, δm is small, oscillations may start during or after annihilations freeze-out, leading to an interesting new phenomenology modifying the final DM relic abundance, a situation that has not yet been studied in detail.

Let us first consider the case where DM is a fermion and both Majorana and Dirac masses are present. The general mass lagrangian using the Weyl spinors X_L and X_R is given by

$$- \mathcal{L}_{mass} = m (\overline{X_R} X_L + \overline{X_L} X_R) + \Delta (\overline{X_L} (X_L)^c + \overline{(X_R)^c} X_R) \quad (1)$$

where we have assumed $\Delta_L = \Delta_R = \Delta$ for simplicity. In matricial form it becomes

$$- \mathcal{L}_{mass} = \frac{1}{2} \overline{((X_L)^c \ X_R)} \begin{pmatrix} \Delta & m \\ m & \Delta \end{pmatrix} \begin{pmatrix} X_L \\ (X_R)^c \end{pmatrix} + h.c. \quad (2)$$

The matrix $\mathcal{M} = \begin{pmatrix} \Delta & m \\ m & \Delta \end{pmatrix}$ is symmetric due to the anti commutation properties of the fermion fields and the properties of the charge conjugation matrix C [53]. It has mass eigenvalues $m_{1/2} = m \mp \Delta$, associated with mass eigen states $X_{1/2,L} = (X_R)^c \mp X_L$, $X_{1/2,R} = X_R \mp X_L^c$. We can then deduce the effective hamiltonian in the non-relativistic limit in the (X, X^c) basis:

$$\mathcal{H} = \mathcal{U}^{-1} \begin{pmatrix} m - \Delta & 0 \\ 0 & m + \Delta \end{pmatrix} \mathcal{U} = \begin{pmatrix} m & \Delta \\ \Delta & m \end{pmatrix} \quad (3)$$

A non-zero value for Δ is responsible for the oscillations between X and X^c . We will typically be considering the situation $\Delta \ll m$ ³.

A similar analysis applies to a complex scalar field which splits into two quasi-degenerate real scalars. A well-known example is the sneutrino that carries the same lepton numbers as the neutrino and is distinct from its antiparticle, the anti-sneutrino. In the presence of a lepton number violation (for instance through the $\tilde{l}HH$ operator, where H is the Higgs field) sneutrinos can mix with anti-sneutrinos since no other quantum numbers forbid the mixing [54, 55, 56, 57]. The mass squared matrix can be written for a single generation as

$$\mathcal{L}_{mass} = \frac{1}{2} (\varphi, \varphi^*)^* \begin{pmatrix} m^2 & \Delta^2/2 \\ \Delta^2/2 & m^2 \end{pmatrix} \begin{pmatrix} \varphi \\ \varphi^* \end{pmatrix} \quad (4)$$

The mass eigenvalues are now $m_{1/2}^2 = m^2 \mp \Delta^2/2$ so that for $\Delta \ll m$, $m_2 - m_1 \approx \Delta^2/(2M)$. Therefore, in the bosonic case, the mass splitting between the mass eigenstates is given by

³Note that one can easily generalize our results to the case where $\Delta_L \neq \Delta_R$. In terms of $\Delta_+ = \Delta_L + \Delta_R$ and $\Delta_- = \Delta_L - \Delta_R$, the mass eigenstates become $m_{1/2} = \frac{1}{2}(\Delta_+ \mp \sqrt{\Delta_-^2 + 4m^2})$. Since we work in the regime $\Delta_L, \Delta_R \ll 1$, one just has to replace Δ in (3) by $\Delta = (\Delta_L + \Delta_R)/2$. As for the mass eigenstates, $X_{1/2,L} = (\frac{\Delta_- \mp \sqrt{\Delta_-^2 + 4m^2}}{2m}, 1)$, they remain almost-equal admixtures of X and X^c .

the see-saw formula, $\Delta^2/(2M)$, rather than the mass term breaking the DM number, 2Δ , and this factor is what enters in the off-diagonal component of the effective lagrangian. In the (φ, φ^*) basis:

$$\mathcal{H} = \begin{pmatrix} m & \Delta^2/(4M) \\ \Delta^2/(4M) & m \end{pmatrix} \quad (5)$$

Therefore, for our phenomenological analysis, we will use the generic form

$$\mathcal{H} = \begin{pmatrix} m & \delta m \\ \delta m & m \end{pmatrix} \quad \text{where} \quad \delta m = \begin{cases} \Delta & \text{if fermionic DM} \\ \Delta^2/(4M) & \text{if bosonic DM} \end{cases} \quad (6)$$

Note that the lagrangians of the models we are concerned with are similar to the ones of inelastic dark matter [58, 59], although we are considering a much smaller Δ so that at the end we are focussing on different phenomenological properties. Typical examples are either a WIMP interacting with a hidden $U(1)'$ gauge boson or a WIMP charged under $SU(2)_L$ [59, 46]. Both in the fermionic and bosonic cases, it is technically natural to have the ‘Majorana’ mass Δ much smaller than the ‘Dirac’ mass m since Δ violates a global $U(1)_{\text{DM}}$ symmetry, due for instance to the vev of some scalar field and all quantum corrections to Δ are proportional to itself. In our model-independent study, δm is a free parameter which, even if very small, will be scanned over orders of magnitude in the sub-eV range. Still, let us note that a natural value in the fermionic case is obtained from the dimension-5 operator

$$\frac{XXH^\dagger H}{\Lambda} \quad (7)$$

After electroweak symmetry breaking and taking Λ at the Planck scale we obtain the see-saw value $\delta m \sim 10^{-6}$ eV. This value turns out to lead to interesting cosmological effects. In fact, as we will see shortly, if $m \lesssim 10$ TeV, δm should not be larger than ~ 1 eV if we want oscillations to have an effect on the final relic abundance. In the bosonic case, this translates into a bound $\Delta \lesssim 10^{-2}$ GeV, which is less straightforward to explain from an operator

$$\lambda \varphi \varphi H H \quad (8)$$

since that would require $\lambda \lesssim 10^{-8}$. There are however ways to sequester the effects of $U(1)_{\text{DM}}$ breaking, see e.g. [59].

Since the upper edge of cosmologically relevant values for δm may not be so far away from the mass scale of neutrinos, it is tempting to try and link the two. Even when the two scales vary by orders of magnitude, it is worth considering a possible common origin for the Majorana masses of neutrino and dark matter. There is a significant literature which relates neutrino mass and dark matter (e.g. [60] and references therein). There has also been attempts to link DM and neutrinos together with leptogenesis. For instance, in the recent Ref. [37], an extra hidden scalar ϕ couples DM with the right-handed neutrino N . In this class of models, if ϕ acquires a vev , it generates a Majorana mass for DM but also induces a mixing between DM and neutrinos that can lead to DM decay depending on the choice of parameters, in particular on m_N . Alternatively, an earlier interesting possibility was brought up in [61] where a \mathbb{Z}_2 symmetry forbids a vev for the new scalar (an $SU(2)_L$ doublet) and there is no Dirac mass linking ν with N , thus guaranteeing the stability of DM. Nevertheless a Majorana mass can be generated at loop-level. Another explanation for the stability of DM may be that a \mathbb{Z}_2 emerges as an unbroken remnant of a global $U(1)_{B-L}$ [60].

3 Oscillation + annihilation + scattering formalism

Our aim is to study the evolution in time t of the populations of DM particles and their antiparticles $\overline{\text{DM}}$, denoted respectively by n^+ and n^- , which possess an initial asymmetry and are subject to the simultaneous processes of annihilations $\text{DM}\overline{\text{DM}} \rightarrow \text{SM}\overline{\text{SM}}$ (with SM being any Standard Model particle), oscillations $\text{DM} \leftrightarrow \overline{\text{DM}}$ and elastic scatterings $\text{DMSM} \rightarrow \text{DMSM}$. For definiteness, we assume that particles are initially more abundant than antiparticles, i.e. $n^+ > n^-$.

The proper tool to treat this problem, in which a coherent process such as oscillations is overlapping with incoherent processes such as annihilations and scatterings, is provided by the density matrix formalism, originally developed for the case of neutrino oscillations in the Early Universe [62], but which can be adapted to our present needs. One defines a 2×2 matrix, whose diagonal entries correspond to the individual number densities n^+ and n^- and whose off-diagonal entries express the superposition of quantum states $^+$ and $^-$ originated by the oscillations. As is customary, we introduce the comoving densities $Y^\pm \equiv n^\pm/s$, where s is the total entropy density of the Universe, and we follow the evolution in terms of the dimensionless variable $x = m_{\text{DM}}/T$, where m_{DM} is the DM mass and T the temperature. We will therefore work in terms of a *comoving number density matrix*

$$\mathcal{Y}(x) = \begin{pmatrix} Y^+(x) & Y^{+-}(x) \\ Y^{-+}(x) & Y^-(x) \end{pmatrix} \quad (9)$$

(the curly font for \mathcal{Y} will indicate in the following the matrix quantity). We will always be interested in the epoch of radiation domination, during which the Hubble parameter $H(x) = \sqrt{8\pi^3 g_*(x)/90} m_{\text{DM}}^2 x^{-2}/M_{\text{Pl}} = H_m/x^2$ and $t^{-1} = 2H(x)$. In terms of x one also has $s(x) \simeq 2\pi^2/45 g_{*s}(x) m_{\text{DM}}^3 \cdot (1/x^3)$.⁴ Here $g_*(x)$ and $g_{*s}(x)$ are the effective relativistic degrees of freedom. We define the ' notation as

$$' \equiv \left[1 - \frac{x dg_*(x)/dx}{4 g_*(x)} \right]^{-1} \times \frac{d}{dx} = \frac{1}{x H(x)} \times \frac{d}{dt} \quad (10)$$

Neglecting the x -dependence of g_* is often an acceptable approximation; for completeness, however, we keep the factor in square brackets in eq. (10) in all our computations.

We will now write explicitly the full density matrix equation that we consider. For a better illustration and understanding, we will discuss each piece of the equation (and the parameters that they contain) one by one in the next subsections, considering in turn a situation with only annihilations and no oscillations nor elastic scatterings, a situation with oscillations only, then combining oscillations and annihilations and finally including the elastic scattering as well. In the cases in which it is possible and convenient, we will deduce from the matricial form of the equation the more familiar Boltzmann equations for Y^+ and Y^- . The evolution equation for the density matrix \mathcal{Y} reads

$$\begin{aligned} \mathcal{Y}'(x) = & -\frac{i}{x H(x)} \left[\mathcal{H}, \mathcal{Y}(x) \right] \\ & -\frac{s(x)}{x H(x)} \left(\frac{1}{2} \left\{ \mathcal{Y}(x), \Gamma_a \bar{\mathcal{Y}}(x) \Gamma_a^\dagger \right\} - \Gamma_a \Gamma_a^\dagger \mathcal{Y}_{\text{eq}}^2 \right) \\ & -\frac{1}{x H(x)} \left\{ \Gamma_s(x), \mathcal{Y}(x) \right\}. \end{aligned} \quad (11)$$

⁴The \simeq sign in the latter relation just reminds that the total entropy density is dominated by the entropy density in relativistic degrees of freedom, in a very good approximation.

On the right hand side, the first term accounts for oscillations, the second for annihilations and the third for elastic scatterings. The initial conditions read $Y_0^\pm \equiv Y^\pm(x_0) = Y_{\text{eq}}(x_0) e^{\pm\xi_0}$ and $Y^{+-}(x_0) = Y^{-+}(x_0) = 0$, at an initial time x_0 (in practice we usually choose $x_0 = 5$, early enough to be able to follow the whole subsequent evolution, but not too early, so that we are always dealing with non-relativistic DM particles). Here Y_{eq} denotes an equilibrium comoving density $Y_{\text{eq}} = \frac{45}{2\pi^4} \left(\frac{\pi}{8}\right)^{1/2} \frac{g}{g_{*s}} x^{3/2} e^{-x}$, where g is the number of internal degrees of freedom (equal to 2 both for the fermionic and the scalar DM case). The actual equilibrium comoving densities for the $+$ and $-$ species are respectively $Y_{\text{eq}}^+ = Y_{\text{eq}} e^{+\xi}$, $Y_{\text{eq}}^- = Y_{\text{eq}} e^{-\xi}$, where $\xi = \mu/T$ with μ being the chemical potential. Since they enter only as the product (see below), the chemical potential disappears from the equations. It is also useful to introduce the parameter $\eta_0 = Y_0^+ - Y_0^-$, which represents the initial DM – $\overline{\text{DM}}$ asymmetry and is related to ξ_0 as $\xi_0 = \text{arcsinh}(\eta_0/(2Y_{\text{eq}}(x_0)))$.

3.1 Annihilations only

In the case with annihilations only, the density matrix equation in eq. (11) reduces to

$$\mathcal{Y}'(x) = -\frac{s(x)}{x H(x)} \left(\frac{1}{2} \left\{ \mathcal{Y}(x), \Gamma_a \bar{\mathcal{Y}}(x) \Gamma_a^\dagger \right\} - \Gamma_a \Gamma_a^\dagger \mathcal{Y}_{\text{eq}}^2 \right). \quad (12)$$

The right hand side, in particular with its anti-commutator structure, reproduces the more detailed collision integrals and once the integral over the phase space of incoming and outgoing particles has been performed, as discussed in [62]. We neglect the effects related to the quantum-statistical distribution of particles (e.g. Fermi-blocking factors). Here Γ_a is a diagonal matrix (actually proportional to the identity in the case at hand) defined in such a way that $\Gamma_a \Gamma_a^\dagger = \langle \sigma v \rangle \mathbb{I}$, where $\langle \sigma v \rangle$ is the thermally averaged annihilation cross section. $\langle \sigma v \rangle$ admits the usual expansion in even powers of the velocity v of the DM particles

$$\langle \sigma v \rangle = \sigma_0 + \sigma_1 \langle v \rangle^2 + \mathcal{O}(v^4), \quad (13)$$

For simplicity, we will always assume s -wave annihilations in the following, which amounts to keep only the first term of the expansion. $\bar{\mathcal{Y}}$ is the charge-conjugated matrix of \mathcal{Y} , i.e. the same quantity as the latter but with the role of particles and antiparticles flipped: $\bar{\mathcal{Y}} = \text{CP}^{-1} \cdot \mathcal{Y} \cdot \text{CP}$, where $\text{CP} = i\sigma_2 = \begin{pmatrix} 0 & 1 \\ -1 & 0 \end{pmatrix}$. Finally, the matrix $\mathcal{Y}_{\text{eq}}^2$ reads $\mathcal{Y}_{\text{eq}}^2 = \begin{pmatrix} Y_{\text{eq}}^2 & 0 \\ 0 & Y_{\text{eq}}^2 \end{pmatrix}$.

In solving eq. (12), the off-diagonal components remain identically zero and the whole information on the evolution of the system is encoded in the equations for the diagonal components Y^\pm . Such equations can then be recast in the more familiar Boltzmann form [63]:

$$Y^{\pm\prime}(x) = -\frac{\langle \sigma v \rangle s(x)}{x H(x)} \left[Y^+(x) Y^-(x) - Y_{\text{eq}}^2(x) \right]. \quad (14)$$

It is now straightforward to solve the equations (12) (or, equivalently, eq. (14), as it has been done in [50, 51]). We show in fig.1 (upper left panel) the result in the specific case $\eta_0 = \eta_B = 1.02 \cdot 10^{-10}$ (the latter being the value of the baryonic asymmetry, see e.g. [1])⁵

⁵Note that we have defined here the quantities η , for DM and for baryons, in terms of the ratio of the difference of number densities with entropy s : $\eta = (n - \bar{n})/s$. This notation is not to be confused with the one (sometimes also denoted η) involving the ratio with the photon number density. In this latter notation, the baryon to photon ratio $(n_B - \bar{n}_B)/n_\gamma \simeq n_B/n_\gamma$ equals the familiar value $6.18 \cdot 10^{-10}$ [1].

and where we have taken a large annihilation cross section. Let us comment on the main qualitative features. At small x , the presence of a primordial asymmetry is irrelevant and both comoving densities follow essentially the equilibrium curve. Freeze-out happens when the system runs out of targets, and then the absolute value of Y^+ (assumed to be the most abundant species) approaches η_0 : Y^+ sits on a plateau while the contribution of Y^- can be neglected. As anticipated, therefore, in this typical aDM configuration the most relevant parameter is the initial asymmetry $\eta_0 = \eta_B$: it sets the asymptotic number density⁶ and thus, in order to obtain the correct Ω_{DM} , forces m_{DM} to be $\mathcal{O}(5 \text{ GeV})$ (4.5 GeV in the plot).

For illustration one can also define the sum and the difference of the comoving number densities

$$\Sigma(x) = Y^+(x) + Y^-(x), \quad \Delta(x) = Y^+(x) - Y^-(x), \quad (15)$$

In terms of these quantities, the Boltzmann equations read

$$\begin{cases} \Sigma'(x) = -2 \frac{\langle \sigma v \rangle s(x)}{x H(x)} \left[\frac{1}{4} \left(\Sigma^2(x) - \Delta^2(x) \right) - Y_{\text{eq}}^2(x) \right], \\ \Delta'(x) = 0, \end{cases} \quad (16)$$

which clearly shows that the difference Δ between the populations remains constant (and equal to the initial condition η_0); on the other hand, the total population Σ of $+$ and $-$ particles decreases, due to annihilations. At late times, Y_{eq} is negligible and Σ is attracted towards $\Delta = \eta_0$.

3.2 Oscillations only

We consider next the restricted case in which there are only $\text{DM} \leftrightarrow \overline{\text{DM}}$ oscillations in the system, without annihilations nor scatterings with the plasma. Eq. (11) reduces in this case to the simple form

$$\mathcal{Y}'(x) = -\frac{i}{x H(x)} [\mathcal{H}, \mathcal{Y}(x)]. \quad (17)$$

where \mathcal{H} is the Hamiltonian of the system, which, as discussed in Sec. 2, we parametrize as

$$\mathcal{H} = \begin{pmatrix} m_{\text{DM}} & \delta m \\ \delta m & m_{\text{DM}} \end{pmatrix}. \quad (18)$$

The system of four coupled equations for the individual entries of the matrix \mathcal{Y} can be explicitly solved analytically. The off-diagonal components can be plugged in the equations for the diagonal components Y^\pm and one finds that those correspond to the following familiar Boltzmann equations:

$$\begin{cases} Y^{+'}(x) = -\frac{\Gamma_{\text{osc}}(x)}{x H(x)} [Y^+(x) - Y^-(x)], \\ Y^{-'}(x) = -Y^{+'}(x), \end{cases} \quad (19)$$

⁶Note that we are assuming that any process changing the DM-number (such as e.g. weak sphalerons, in models in which the DM-number is related to the ordinary baryon number) is already switched off by the time of freeze-out, so that we can consider η_0 as an actual constant in the subsequent evolution. This could be invalid for very large DM masses ($\gtrsim 10 \text{ TeV}$), for which freeze-out happens early.

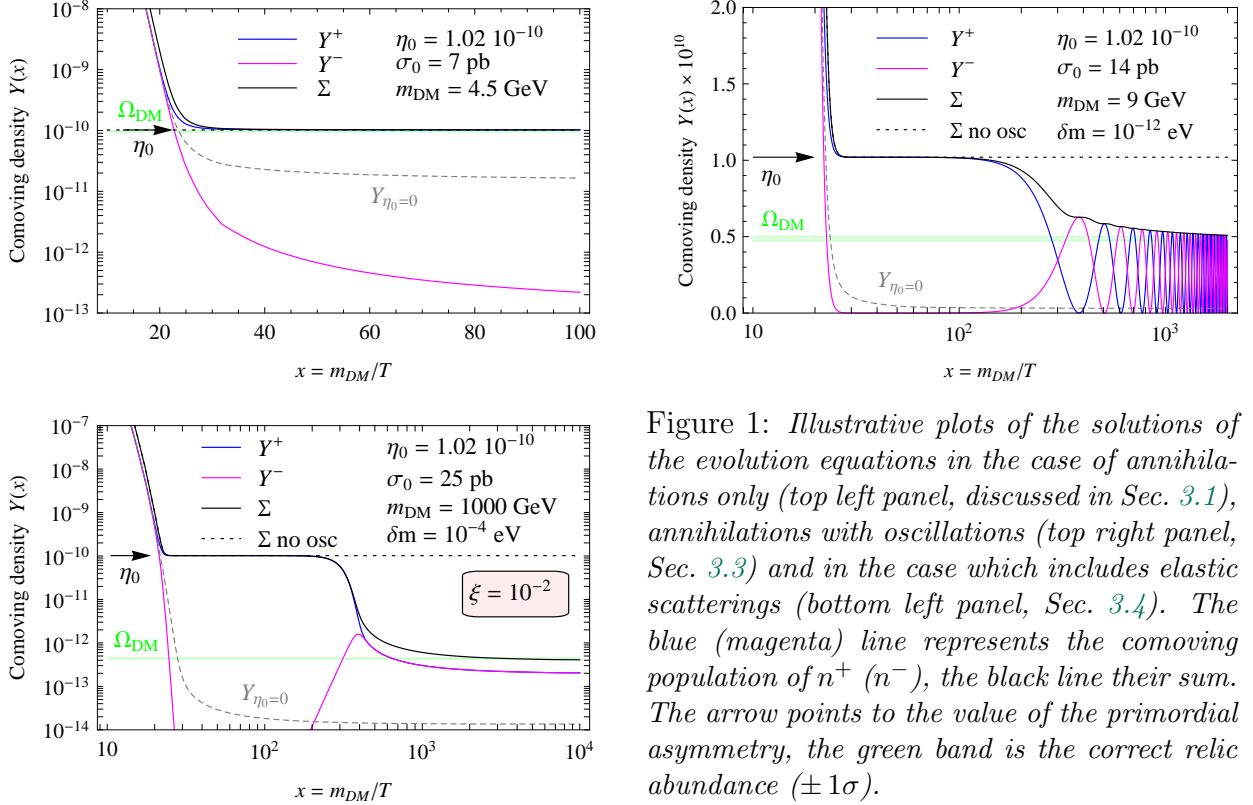


Figure 1: Illustrative plots of the solutions of the evolution equations in the case of annihilations only (top left panel, discussed in Sec. 3.1), annihilations with oscillations (top right panel, Sec. 3.3) and in the case which includes elastic scatterings (bottom left panel, Sec. 3.4). The blue (magenta) line represents the comoving population of n^+ (n^-), the black line their sum. The arrow points to the value of the primordial asymmetry, the green band is the correct relic abundance ($\pm 1\sigma$).

with the same initial conditions as for eq. (11) and where the oscillation rate is defined as

$$\Gamma_{\text{osc}}(x) = \delta m \tan\left(\frac{\delta m}{H(x)}\right). \quad (20)$$

These can also be written in terms of Σ and Δ as

$$\begin{cases} \Sigma'(x) = 0, \\ \Delta'(x) = -2 \frac{\Gamma_{\text{osc}}(x)}{x H(x)} \Delta(x). \end{cases} \quad (21)$$

It is now Σ which is constant in time, since oscillations exchange particle with antiparticle but conserve the total number of bodies, while $\Delta(x)$ follows an oscillatory behaviour.

In the absence of interactions with the plasma, the probability that a DM particle becomes a $\overline{\text{DM}}$ particle at time t is simply $P_{\text{osc}}^{+-}(t) = \sin^2(\delta m t)$. Oscillations start when $H(x) \lesssim \delta m$ (i.e $T \lesssim \sqrt{\delta m M_{\text{Pl}}}$). Slightly more precisely, one can define x_{osc} via the condition $\delta m x_{\text{osc}}^2 / H(m_{\text{DM}}) \simeq 2\pi$, which gives

$$x_{\text{osc}} \simeq \left(\frac{8\pi^3}{90} g_*\right)^{1/4} \frac{1}{\sqrt{M_{\text{Pl}}}} \frac{m_{\text{DM}}}{\sqrt{\delta m}} \approx 2 \cdot 10^{-4} \left(\frac{m_{\text{DM}}}{10 \text{ GeV}}\right) \left(\frac{\text{eV}}{\delta m}\right)^{1/2}. \quad (22)$$

This equation is plotted in Fig. 2, showing that a large range of possibilities is open, depending on the values of the DM mass and of the δm parameter. We will later see how this relation is modified by the presence of annihilations and elastic scatterings.

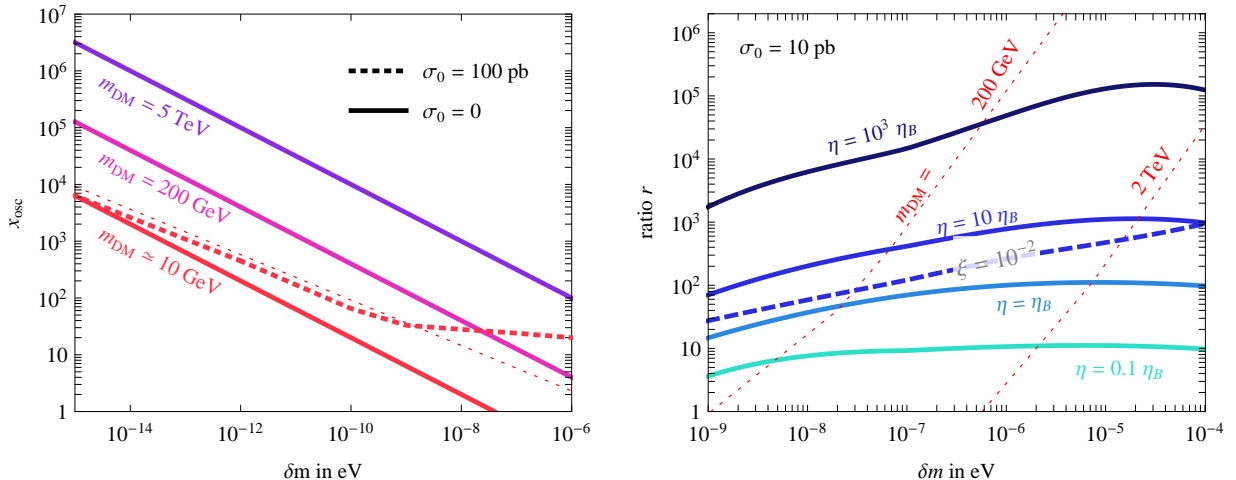


Figure 2: **Left panel:** illustration of the approximate relation in eq. (22) and eq. (25), i.e. the value of x at which oscillations start as a function of δm for a few indicative values of the DM mass. The dotted lines trace the modification to that relation in the case where annihilations are active, see Sec. 3.3. **Right panel:** graphical illustration of the approximate relation in eq. (34), i.e. the efficiency of oscillations in depleting the aDM excess (for definiteness, in the case of no elastic scatterings, i.e. $\xi = 0$, except for the dashed line marked by the label $\xi = 10^{-2}$). The crossings of the diagonal dotted lines with the four solid lines individuate the values of δm for which Ω_{DM} reproduces the correct abundance, for the indicated values of m_{DM} .

3.3 Combining annihilations and oscillations

When combining annihilations and oscillations, the features that we separately highlighted above overlap: initially the total number of particles decreases due to annihilations; later, when oscillations start, they repopulate Y^- at the expense of Y^+ so that annihilations can recouple, thus reducing the sum; as a consequence, in the next ‘cycle’, the total number of Y^+ and Y^- subject to oscillations is reduced, i.e. the amplitude of the oscillation also decreases. The amount by which the amplitude of the oscillations decreases is determined by the amount by which the sum of particles at disposal decreases.

All this is accounted for by eq. (11), that we reproduce here for convenience:

$$\mathcal{Y}'(x) = -i \frac{1}{x H(x)} \left[\mathcal{H}, \mathcal{Y}(x) \right] - \frac{s(x)}{x H(x)} \left(\frac{1}{2} \left\{ \mathcal{Y}(x), \Gamma_a \bar{\mathcal{Y}}(x) \Gamma_a^\dagger \right\} - \Gamma_a \Gamma_a^\dagger \mathcal{Y}_{\text{eq}}^2 \right). \quad (23)$$

This equation can be recast into a set of coupled Boltzmann-like relations, namely:

$$\begin{cases} \Sigma'(x) = -2 \frac{\langle \sigma v \rangle s(x)}{x H(x)} \left[\frac{1}{4} \left(\Sigma^2(x) - \Delta^2(x) - \Xi^2(x) \right) - Y_{\text{eq}}^2(x) \right], \\ \Delta'(x) = \frac{2i \delta m}{x H(x)} \Xi(x), \\ \Xi'(x) = \frac{2i \delta m}{x H(x)} \Delta(x) - \frac{\langle \sigma v \rangle s(x)}{x H(x)} \Xi(x) \Sigma(x). \end{cases} \quad (24)$$

where Ξ corresponds to the difference between off-diagonal elements of the density matrix, $\Xi(x) = Y^{+-}(x) - Y^{-+}(x)$. From this, it is clear that the system cannot be reduced to

simple equations for the two functions Σ and Δ (already defined above). In other words, the interplay of coherent and incoherent processes cannot be thoroughly followed by focussing only on the populations of Y^+ and Y^- , or their sum and difference: one more functional ‘degree of freedom’ is needed.

Some insight can anyhow be learnt by considering the (oversimplified) case featuring oscillations and a *constant* effective rate of annihilations, denoted γ_a , and neglecting variation with x of the total population Σ . In this case, by combining the second and third equations in (24), one arrives at an effective equation $\Delta' \simeq -2\delta m^2/\gamma_a \Delta$, valid in the regime $\gamma_a \gg \delta m$. Contrasted with the second of eq. (21), this shows that, in presence of annihilations, the difference between the populations dims with a rate proportional to $\delta m^2/\gamma_a$, a point to which we will come back later. However, we stress that this simplification does not allow to include all the features of the system. We will stick to the full equation (23) for the numerical solutions in the following.

In figure 1 (top right panel) we show the numerical result of eq. (23) (or, equivalently, eq. (24)) for a specific illustrative case. Like for the top left example in the same figure, we have again taken $\eta_0 = \eta_B$, but here the population Y^+ sits only temporarily on the plateau determined by η_0 . With a value of $\delta m = 10^{-12}$ eV, oscillations start at $x \sim 300$ and we see Y^- being repopulated. Given the relatively large annihilation cross section $\sigma_0 = 14$ pb, annihilations can then promptly resume and the total population Σ decreases. In the later stages, Σ goes through a rapid series of plateaux and drops, until it rests on its asymptotic value, determined by the freeze-out of annihilations. One can therefore have a final $Y_\infty \ll \eta_0$ and obtain the same $\Omega_{\text{DM}} = \rho_{\text{DM}}/\rho_{\text{crit}} = m_{\text{DM}} Y_\infty s/\rho_{\text{crit}}$ with a large DM mass with respect to the standard aDM case. In other words, this example illustrates how, as anticipated in the introduction, Ω_{DM} is no longer determined by η_0 but by the combination of different parameters $\eta_0, m_{\text{DM}}, \delta m, \sigma_0$. We will discuss several illustrative choices for these in Section 4. Note that our formalism allows to follow in detail the oscillatory pattern (evident at large x in fig. 1b). In other approaches in the literature only an effective average of oscillations has been employed (see e.g. [37, 40]). While this may be enough for an estimate of the effect or for the late x behaviour, it may miss the details at the starting-up of oscillations.

Another non trivial effect of the interplay between annihilations and oscillations has to do with the moment of the start of oscillations. While in a purely coherent (albeit expanding) system with only oscillations, as the one we considered in Sec. 3.2, the conversions start at a x_{osc} determined via eq. (22), the addition of annihilations breaks such coherence and effectively delays the picking up of oscillations. In top right panel fig. 1 the effect is barely visible (namely, x_{osc} equals ~ 300 or so, instead of $x_{\text{osc}} \sim 200$ as it would be dictated by eq. (22)), but for larger values of the $\langle\sigma v\rangle$ parameter the suppression and delay of oscillations becomes more important. In terms of the effective simplification discussed below eq. (24), where the relevant time scale is now $\delta m^2/\gamma_a$, we obtain that oscillations start when

$$\begin{aligned}
 x_{\text{osc,ann}} &\simeq \left(\frac{H_m \gamma_a}{2 \delta m^2} \right)^{1/2} \simeq \left(\frac{H_m \sigma_0 s_m \eta_0/2}{\delta m^2} \right)^{1/5} \\
 &\approx 12 \left(\frac{m_{\text{DM}}}{100 \text{ GeV}} \right) \left(\frac{10^{-7} \text{ eV}}{\delta m} \right)^{2/5} \left(\frac{g_{*s}}{10} \sqrt{\frac{g_*}{10}} \frac{\sigma_0}{1 \text{ pb}} \frac{\eta_0}{\eta_B} \right)^{1/5}, \quad (25)
 \end{aligned}$$

where $s_m = s(x = 1)$, in analogy with H_m . In fig. 2 (left panel) we also report, for the specific case of $m_{\text{DM}} = 10$ GeV, the effective value of $x_{\text{osc,ann}}$ for an annihilation cross section of $\sigma_0 = 100$ pb. We plot the value as predicted by eq. (25) (thin dotted line) and as determined numerically (thick dotted line).

3.4 Including elastic scatterings

Dark Matter (and antiDM) particles travel through the dense primordial plasma and elastically scatter on it via $\text{DMSM} \rightarrow \text{DMSM}$ processes, where ‘SM’ denotes any Standard Model particle that is abundant enough in the plasma, i.e. essentially relativistic species. This affects the evolution of the system in two main ways (we follow closely for this discussion the case of neutrino propagation in matter, see e.g. [64]): (i) an effective matter potential V is generated by the coherent interactions and enters in the commutator part of the density matrix equation; (ii) the incoherent scatterings give rise to a rate of interactions γ_s entering in the anti-commutator part.

The whole system is therefore now described by eq. (11) with all pieces included and where

$$\mathcal{H} = \begin{pmatrix} m_{\text{DM}} + V(x) + \Delta V(x) & \delta m \\ \delta m & m_{\text{DM}} + V(x) \end{pmatrix} \quad \text{and} \quad \Gamma_s = \begin{pmatrix} \gamma_s & 0 \\ 0 & \gamma_s \end{pmatrix}. \quad (26)$$

The common terms on the diagonal of \mathcal{H} of course do not have any effect on oscillations, while the difference ΔV does. ΔV represents the effective energy shift of DM versus $\overline{\text{DM}}$ induced by the baryon asymmetry of the medium. Effectively, it leads to a non-maximal mixing angle, thus reducing the oscillation probability in the vacuum P_{osc}^{+-} by a factor $4\delta m^2 / (4\delta m^2 + \Delta V^2)$. For simplicity we assume that δm is not affected by the medium.

The explicit form of ΔV and γ_s depends on the specific interactions of DM with the plasma. Since we are mainly interested in the case of Weakly Interacting dark matter, we mimic them from those of neutrinos. An important point to notice, however, is that the same scatterings we are considering here are also those that would produce signals in DM direct detection experiments, i.e. nuclear or electron recoils in low background set-ups. In order to be consistent with direct detection experiments, therefore, we assume that the DM coupling with matter is suppressed with respect to the weak coupling. On the basis of these observations, we take

$$\Delta V = \xi \sqrt{2} G_{\text{F}} \eta_{\text{B}} (g_{*s}(x) - 2) n_{\text{bos}} \quad \text{and} \quad \gamma_s = \xi^2 \frac{45}{\pi^3} \zeta(5) G_{\text{F}}^2 (g_{*s}(x) - 2) \frac{m_{\text{DM}}^5}{x^5}, \quad (27)$$

where G_{F} is the Fermi constant, $n_{\text{bos}} = 1/\pi^2 \zeta(3) m_{\text{DM}}^3/x^3$ is the number density per degree of freedom of relativistic bosons and $\zeta(n)$ is the Riemann zeta function of n . In the equations above the presence of the factor $(g_{*s}(x) - 2)$ is due to the fact that we take into account that WIMP DM scatters on all the relativistic degrees of freedom (counted by $g_{*s}(x)$) except for photons. Also, by using η_{B} in the expression for ΔV , we are implicitly assuming that all relativistic SM species share the same asymmetry, equal to the baryonic one.⁷

⁷Notice that no term proportional to the DM asymmetry itself is present, since the DM and $\overline{\text{DM}}$ population is Boltzmann suppressed in the regimes of our interest. As a consequence, there is no feedback of the evolution of the DM asymmetry into ΔV (such a feedback is instead present in the case of relativistic neutrinos in the Early Universe).

The parameter ξ expresses the suppression of the Fermi constant due to the fainter DM coupling with matter, as discussed above. Direct detection experiments impose $\xi \lesssim 10^{-2}$. On the other hand, one can check that for $\xi \ll 10^{-3}$ the presence of scatterings has essentially no effect on the system. We will therefore consider in this work two main cases:

- (a) $\xi \equiv 0$ (i.e. no scatterings), in which case the system reduces to the one discussed in Sec. 3.3; this scenario makes more evident the effect of oscillations and maximizes their importance.
- (b) $\xi = 10^{-2}$, the maximum allowed value, which makes elastic scatterings, besides annihilations and oscillations, important for the evolution of the DM and $\overline{\text{DM}}$ populations. For large scattering, oscillations are damped, as in the case of standard neutrino mixing in the early universe.

We stress again that eq.s (27) are just choices made for definiteness, since we lack a detailed model of the interactions of DM with SM matter. For instance, if the DM particle couples only to other dark states which ultimately decay to SM ones, ΔV and γ_s are expected to be small. For another instance, if DM is leptophilic and couples only to leptons, then the relevant asymmetry η in ΔV would be the leptonic one, which is poorly constrained. Our formalism allows us to explore most of the possible parameter space while remaining model-independent.

Finally, note that in order to reproduce the correct physical system with the last anti-commutator in eq. (11) (which is an approximation to more detailed expressions of the collision integrals [62]), one needs to forbid the terms proportional to γ_s in the equations for the diagonal components of \mathcal{Y} , as commonly done in the literature. This guarantees that elastic scatterings do not have the effect of depleting the populations of Y^+ and Y^- .

As done in the previous Subsections, one can derive a set of Boltzmann-like equations from the matrix equation in eq. (11) with eq. (26). They read

$$\left\{ \begin{array}{l} \Sigma'(x) = -2 \frac{\langle \sigma v \rangle s(x)}{x H(x)} \left[\frac{1}{4} \left(\Sigma^2(x) - \Delta^2(x) - \Xi^2(x) - \Pi^2(x) \right) - Y_{\text{eq}}^2(x) \right], \\ \Delta'(x) = \frac{2i \delta m}{x H(x)} \Xi(x), \\ \Xi'(x) = \frac{2i \delta m}{x H(x)} \Delta(x) - \frac{i \Delta V}{x H(x)} \Pi(x) - \frac{\gamma_s}{x H(x)} \Xi(x) - \frac{\langle \sigma v \rangle s(x)}{x H(x)} \Xi(x) \Sigma(x), \\ \Pi'(x) = -\frac{i \Delta V}{x H(x)} \Xi(x) - \frac{\gamma_s}{x H(x)} \Pi(x). \end{array} \right. \quad (28)$$

Yet one more functional degree of freedom coupled to the others, the function $\Pi(x) = Y^{+-}(x) + Y^{-+}(x)$, has to be introduced. The interplay of the coherent and incoherent processes (annihilations and scatterings) can thus be thoroughly followed by using the full density matrix formalism, either recast in the form of eq. (28) or, more conveniently, in the form of eq. (11), to which we will adhere in the following.

In order to understand qualitatively the impact of adding incoherent scatterings on the evolution of the populations of DM particles and antiparticles, we can consider the (oversimplified) case of a system featuring oscillations and a *constant* γ_s . We neglect ΔV and we switch off annihilations for simplicity. In this case the matrix equation in eq. (11)

schematically reads $\mathcal{Y}' = -i/(xH)\left([\mathcal{H}, \mathcal{Y}] - \{\Gamma_s, \mathcal{Y}\}\right)$. Proceeding in the same way as discussed in Sec. 3.2, this equation can be recast into the same pair of coupled Boltzmann equations in eq. (19), *but* with a more complicated $\Gamma_{\text{osc}} = 2\delta m^2/(\gamma_s + \omega \coth(\omega/2H(x)))$, where $\omega = \sqrt{\gamma_s^2 - 4\delta m^2}$. It is then straightforward to recognize two limits. If elastic scatterings are negligible ($\gamma_s \ll \delta m$) then $\Gamma_{\text{osc}} \rightarrow \delta m \tan(\delta m/H(x))$, reducing the system to the case with pure oscillations discussed in Sec. 3.2. If instead elastic scatterings are dominant ($\gamma_s \gg \delta m$), then at late times Γ_{osc} approaches a constant value $\Gamma_{\text{osc}} \rightarrow 2\delta m^2/\gamma_s$. In this situation, the eq.s (19) describe a system of Y^+ and Y^- densities that are driven, with a strength determined by $\Gamma_{\text{osc}} = 2\delta m^2/\gamma_s$, one towards the other. In other words, oscillations are damped away and the comoving densities tend asymptotically to their average value. Note that in this case, we recover an equation which is often used in the literature e.g. in [37, 40, 65, 66]: $Y^{+'}(x) = -\frac{\langle P \rangle \gamma_s}{xH(x)} [Y^+(x) - Y^-(x)]$, namely the transfer rate is just the averaged oscillation probability, $\langle P \rangle = \gamma_s \int_0^\infty dt e^{-\gamma_s t} \sin^2 \delta m t$, multiplied by the interaction rate. In the full case, which includes x -dependent scattering rates and also annihilations, a comparably simple analytic understanding is not possible, but these general features are preserved, as we move to illustrate next.

In figure 1 (bottom left panel) we show the outcome of the numerical resolution of eq. (11) with eq. (26), for a specific illustrative case. As in the previous examples, we have again taken $\eta_0 = \eta_B$. In this case, despite the large δm , oscillations do not pick up until late, as they are suppressed by the incoherent scatterings. Hence the total density of DM sits for a long time on the familiar plateau. When oscillations do rise (and annihilations restart), barely one oscillating cycle can be seen before they are damped and Y^+ and Y^- settle on their asymptotic common value. This illustrates how the inclusion of incoherent scatterings opens a quite different regime: oscillations still have the role of re-symmetrizing the populations allowing for a partial wash-out of the frozen asymmetry, but the ranges of parameters involved are different.

We conclude this section by commenting on the quantitative delay of the start of oscillations due to the presence of elastic scatterings. Following the same arguments as in Sec. 3.3, it is easy to see that now one has approximately

$$\begin{aligned} x_{\text{osc,scatt}} &\simeq \left(\frac{H_m \gamma_s}{2\delta m^2}\right)^{1/2} \simeq \left(\frac{H_m \gamma_s(x=1)}{\delta m^2}\right)^{1/7} \\ &\approx 130 \left(\frac{m_{\text{DM}}}{100 \text{ GeV}}\right) \left(\frac{10^{-7} \text{ eV}}{\delta m}\right)^{2/7} \left(\left(\frac{g_*}{10}\right)^{3/2} \frac{\xi}{10^{-2}}\right)^{1/7}. \end{aligned} \quad (29)$$

4 Results

We now illustrate with some more examples the physics involved in the solutions of the density matrix equations discussed above by varying the parameters m_{DM} , σ_0 , η_0 , δm and also ξ . In fig. 3 we show the evolution of the comoving dark matter number density in the following cases:

- Case A corresponds to choices similar to those discussed in Sec. 3.3 and already adopted for fig. 1a and is reported here for the sake of comparing with the following cases.

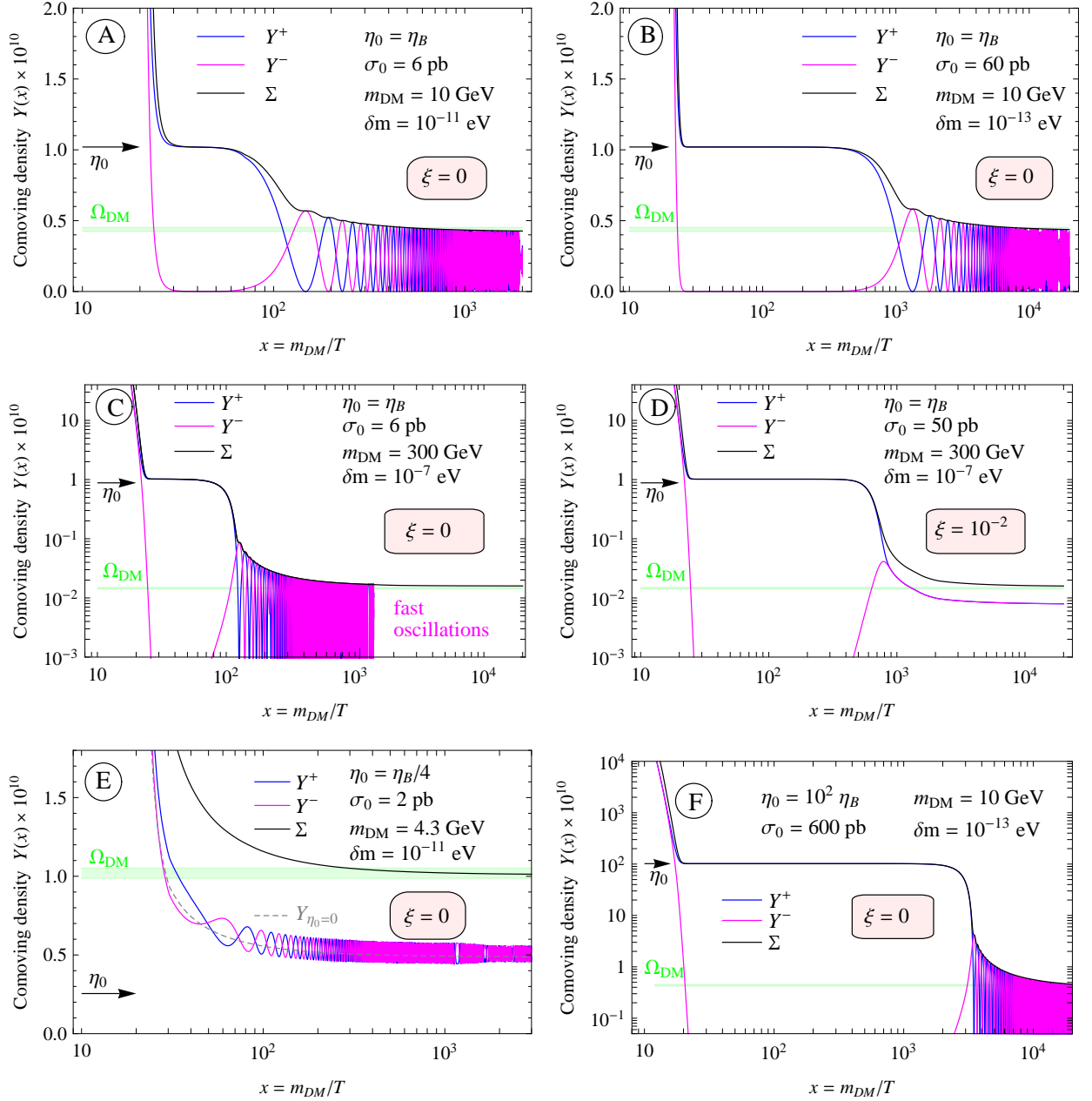


Figure 3: Some illustrative cases of the time evolution of the populations of DM particles and antiparticles. Notations are like in fig. 1, i.e. the blue (magenta) line represents the comoving population of n^+ (n^-), the black line their sum. The arrow points to the value of the primordial asymmetry, the green band is the correct relic abundance ($\pm 1\sigma$). Notice that some plots have linear scale while other have logarithmic ones, depending on structure which is necessary to show. See text for more details.

- In Case B we keep the same m_{DM} as in A, but we adopt a much smaller δm . The comoving population of DM therefore sits for a longer time on the plateau determined by the initial asymmetry η_0 . However, when oscillations eventually start, annihilations (which have a larger cross section of 60 pb) recouple and can lead to the correct relic abundance. Case B displays therefore the same physics as in A, but delayed in time.

Pursuing along this direction, long plateaux can be obtained: an even smaller δm would push the start of oscillations further away and a larger σ_0 would be needed to keep annihilations active that late.

- In case C, we keep instead the same annihilation cross section as in A, but we move to a higher, roughly weak-scale value of the DM mass, $m_{\text{DM}} = 300 \text{ GeV}$. The correct relic abundance is achieved by starting oscillations earlier than in A, i.e. by choosing a much larger δm .
- Case D corresponds to same situation as C (in terms of m_{DM} and δm), except that now we include elastic scatterings ($\xi = 10^{-2}$). The effect of incoherent scatterings that delay and damp the oscillations is very much apparent with respect to case C. A larger cross section is needed to keep the annihilations active at late times and thus reach the right abundance.
- Case E, on the other hand, illustrates a situation which is similar to the standard thermal freeze-out case, despite the presence of an initial asymmetry and of oscillations. Y^+ and Y^- oscillate around the standard solution (in dashed gray, computed for one species only). We have assumed, for this case, a smaller initial asymmetry.
- Case F corresponds to a situation in which a very large initial asymmetry (equal to $10^2 \eta_B$) is assumed. Having adopted a small δm , oscillations start late but nevertheless they eventually bring the abundance to the right value. Like for case B, therefore, the comoving density spends a long time on a value which is, in this case, much larger than the final one.

We systematize and summarize our results by showing the contour lines corresponding to the correct DM abundance in the $(m_{\text{DM}}, \sigma_0)$ plane in Fig. 4. The orange solid line (labelled η_B) corresponds to the standard aDM scenario. By changing the values of δm and η_0 we can open much more of the parameter space, towards larger m_{DM} and larger σ_0 .

Before we move to discuss the constraints on this same parameter space, we want to provide some approximate analytic expressions that help in identifying the general features of the solutions.

First, we want to obtain an estimate of the asymptotical value of $\Sigma = Y^+ + Y^-$, which determines the DM abundance today via $\Omega_{\text{DM}}(x \rightarrow \infty) = m_{\text{DM}} \Sigma(x \rightarrow \infty) s / \rho_{\text{crit}}$, where s here denotes the entropy density today. We focus first on the case with elastic scatterings, $\xi = 10^{-2}$, but neglecting ΔV . By solving in an approximate semi-analytic way the system of equations, we are able to obtain an expression for $\Omega_{\text{DM}}(x \rightarrow \infty)$ as a function of all the parameters of the system. It reads

$$\Omega_{\text{DM}}(x \rightarrow \infty) \simeq \frac{m_{\text{DM}} s}{\rho_{\text{crit}}} \eta_0 \left(1 + \frac{1}{12.2} \frac{g_{*s,\infty}}{g_{*,\infty}^{4/7}} \left(\pi^2 \frac{\delta m^2 M_{\text{Pl}}^8}{\xi^2 \gamma_{s,0}} \right)^{1/7} \text{Gamma} \left[\frac{6}{7} \right] \sigma_0 \eta_0 \right)^{-1}, \quad (30)$$

where $\gamma_{s,0} = 45/\pi^3 \zeta(5) G_{\text{F}}^2 (g_{*s} - 2)$ corresponds to the normalization factors of the scattering rate γ_s in eq. (27) and $g_{*(s),\infty}$ denotes quantities evaluated today. This approximation holds when, before the onset of oscillations, all Y^- annihilate and the energy density of the Universe is dominated by $Y^+ \sim \eta_0$. It therefore becomes unreliable for large δm . In addition, for large annihilation cross sections (indicatively $\sigma_0 > 100 \text{ pb}$) the manipulations

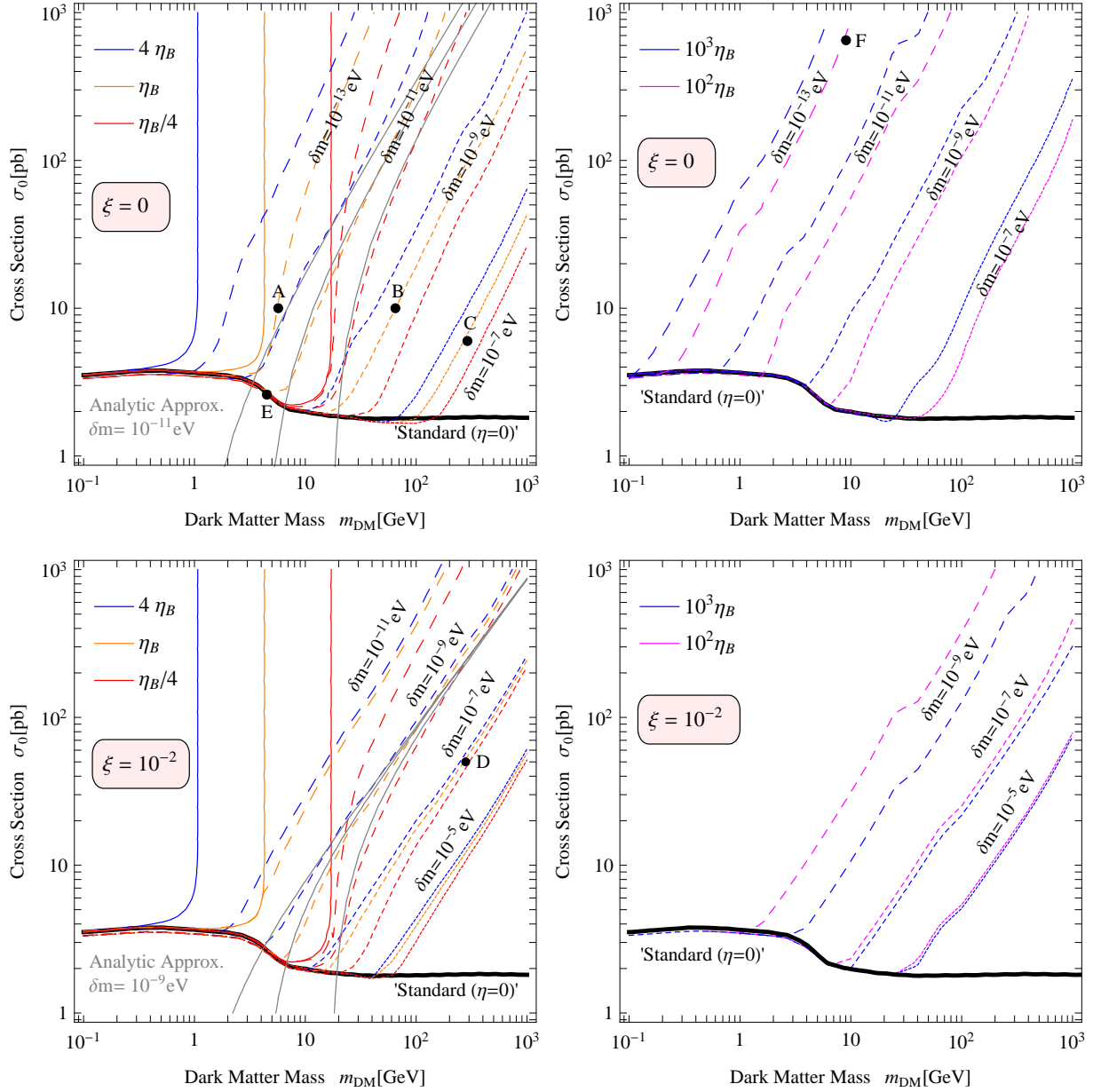


Figure 4: Contour lines along which a correct $\Omega_{\text{DM}} h^2$ can be obtained, for various values of the initial asymmetry η_0 (various colors) and several values of the oscillation parameter δm (labelled lines marked by different dashings). The solid thick black line at the bottom represents the standard case ($\eta = 0, \delta m = 0$). The labelled points (A to F) refer to the cases shown in Fig. 3. **Top panels:** Oscillations and annihilations only, i.e. with $\xi = 0$. **Bottom panels:** Adding elastic scatterings, i.e. with $\xi = 10^{-2}$. The **left panels** consider initial asymmetries equal or close to the baryonic one. The **right panels** focus on large initial asymmetries. The faint gray lines correspond to the semi-analytic approximations in eq. (30) and eq. (33).

leading to eq. (30) do not hold and thus this approximation fails. Within this region of validity, we can readily identify two limits. In the limit of no oscillations ($\delta m \rightarrow 0$), eq. (30) reduces to the usual expression in Asymmetric Dark Matter scenarios:

$$\Omega_{\text{DM}}(x \rightarrow \infty) \simeq \frac{m_{\text{DM}} s}{\rho_{\text{crit}}} \eta_0. \quad (31)$$

At the other extreme, when the second term in brackets in eq. (30) dominates, we have

$$\Omega_{\text{DM}}(x \rightarrow \infty) \simeq \frac{m_{\text{DM}} s}{\rho_{\text{crit}}} \frac{1}{\frac{1}{12.2} \frac{g_{*,\infty}^{4/7}}{g_{*,\infty}^{4/7}} \left(\pi^2 \frac{\delta m^2 M_{\text{Pl}}^8}{\xi^2 \gamma_{s,0}} \right)^{1/7} \text{Gamma} \left[\frac{6}{7} \right] \sigma_0}. \quad (32)$$

In this limit, the dependence on η_0 cancels out. Indeed, in fig. 4, lower left panel, we observe a degeneracy of the curves corresponding to different initial asymmetries, for the largest δm values. For the case without elastic scatterings ($\xi = 0$), in a similar way we obtain the equivalent of eq. (30):

$$\Omega_{\text{DM}}(x \rightarrow \infty) \simeq \frac{m_{\text{DM}} s}{\rho_{\text{crit}}} \eta_0 \left(1 + \frac{1}{5.1} \frac{g_{*,\infty}^{4/5}}{g_{*,\infty}^{3/5}} \left(\frac{\delta m^2 M_{\text{Pl}}^6}{\pi} \right)^{1/5} \text{Gamma} \left[\frac{4}{5} \right] (\sigma_0 \eta_0)^{4/5} \right)^{-1}. \quad (33)$$

In this case, the asymptotic value of Ω_{DM} does carry a more significant residual dependence on η_0 , which indeed we see in figure 4 (upper left panel). We superimpose the contours determined by eq. (30) and eq. (33) to the numerical contours in fig. 4, for one choice of δm . We see that the agreement is good within the ranges of validity.

As a second point, we want to quantify the amount by which the parameter space of Asymmetric Dark Matter opens up due to the introduction of oscillations. For this purpose we can define the ratio

$$r_{\delta m}(\sigma_0, \eta_0) \equiv \frac{\Omega_{\text{DM}} h^2|_{\delta m=0}}{\Omega_{\text{DM}} h^2} \quad (34)$$

where the numerator expresses the DM abundance that would occur in a standard aDM scenario characterized by $(m_{\text{DM}}, \sigma_0, \eta_0)$ if oscillations were not present, while the denominator expresses the same quantity when oscillations (with parameter δm) are switched-on. r therefore quantifies how much we can reduce the DM density by introducing oscillations. When in the denominator we select the value of δm that gives the correct relic abundance $\Omega_{\text{DM}} h^2 \simeq 0.11$, r characterizes therefore the amount of overclosure of the Universe which we would have in the absence of oscillations. We plot r in fig. 2. We work for definiteness in the case with no elastic scatterings ($\xi = 0$), but we do show a line in the case with scatterings (marked $\xi = 10^{-2}$). We also indicate some values in specific points on the iso-lines in fig. 6, in this case both for $\xi = 0$ and $\xi = 10^{-2}$. We see that r can reach very large values, i.e. oscillations can be very efficient in depleting the DM excess.

One could also wonder whether δm can be indefinitely large in these set-ups. This is of course not the case: for too large δm oscillations start too early and symmetrize the dark sector such that decoupling proceeds as in the standard thermal freeze-out scenario. For instance, case E in fig. 3 illustrates a critical case in which oscillations begin somewhat precisely at the right moment to thwart the impact of the asymmetry and drive the evolution along the usual freeze-out history. It can therefore also be useful to explicitly define δm_{max} as the value of δm below which the new phenomena described here arise. The determination

of the value of δm_{\max} which is relevant in the different scenarios is of course tightly related to the identification of the effective start of oscillations x_{osc} , which we have discussed in the different cases of Sec. 3. For the case of oscillations only (neglecting elastic scatterings and annihilations), one obtains

$$\begin{aligned}\delta m_{\max} &\simeq 2\pi H(m)/x_{\text{decoupl, asym.}}^2 \\ &\sim 10^{-11} \sqrt{g_*} (m_{\text{DM}}/1 \text{ GeV})^2 \text{ eV},\end{aligned}\tag{35}$$

where the numerical estimate in the last step is obtained by neglecting a small change in the value of $x = m_{\text{DM}}/T$ at decoupling, in our scenario with respect to the standard case, i.e. we assumed the standard value $x_{\text{decoupl, asym.}} \approx x_{\text{decoupl, std.}} \sim 20$. We see, that for heavy DM, with mass ~ 1 TeV, already for $\delta m \leq 10^{-5}$ eV oscillations affect the decoupling history. For lighter DM, δm is accordingly smaller. In the case with annihilations or scatterings, the relation above is modified as discussed in Sec. 3. One has

$$\begin{aligned}\delta m_{\max} &\simeq \left(\frac{H_m \gamma_{\text{a,s}}}{x_{\text{decoupl}}} \right)^{1/2} \\ &\approx 10^{-7} \text{ eV} \sqrt{\frac{g_{*s}}{85} \frac{\sqrt{g_*}}{85} \frac{\sigma_0}{1 \text{ pb}} \frac{\eta_0}{\eta_B} \left(\frac{m_{\text{DM}}}{100 \text{ GeV}} \frac{20}{x_{\text{decoupl}}} \right)^5} \quad \text{if } \gamma_{\text{a}} \gg \gamma_{\text{s}}\end{aligned}\tag{36}$$

$$\approx 4 \cdot 10^{-4} \text{ eV} \sqrt{\left(\frac{g_*}{85} \right)^{3/2} \frac{\xi}{10^{-2}} \left(\frac{m_{\text{DM}}}{100 \text{ GeV}} \frac{20}{x_{\text{decoupl}}} \right)^7} \quad \text{if } \gamma_{\text{s}} \gg \gamma_{\text{a}}\tag{37}$$

where $\gamma_{\text{a,s}}$ is the larger of the effective rates introduced in Sec. 3. Figure 5 illustrates the regions in the parameter plane $\delta m/m_{\text{DM}}$ which are individuated by these approximate arguments.

Another feature of these models worth emphasizing is that the required annihilation cross section always needs to be *higher* than the usual thermal freeze-out value σ_0 . This occurs just because annihilations have to still be active later than in the usual scenario. The parameter space is indeed effectively bound from below at cross sections of the order of 2 pb⁸. High cross sections in the standard case would under-produce Ω_{DM} , while with the asymmetry+oscillation mechanism, we can reach the correct value.

5 Constraints

In the setup we are considering, when oscillations start, annihilations promptly resume. Therefore the parameter space presented above is subject to the usual constraints on annihilating dark matter. Since, in some examples, we are dealing with large annihilation cross sections, these constraints can be particularly significant. We will discuss the constraints coming from the different epochs, and then identify the most stringent ones. We will always work under the assumption that oscillations started much before the epoch considered for the constraint, so that the populations Y^+ and Y^- have already undergone a very large number of oscillation cycles and therefore can be both approximated with their average

⁸Note that as we have two DM species, we have a twice lower number of targets than in the case where DM is its own antiparticle, and therefore cross sections twice higher are needed to have the same annihilation rate.

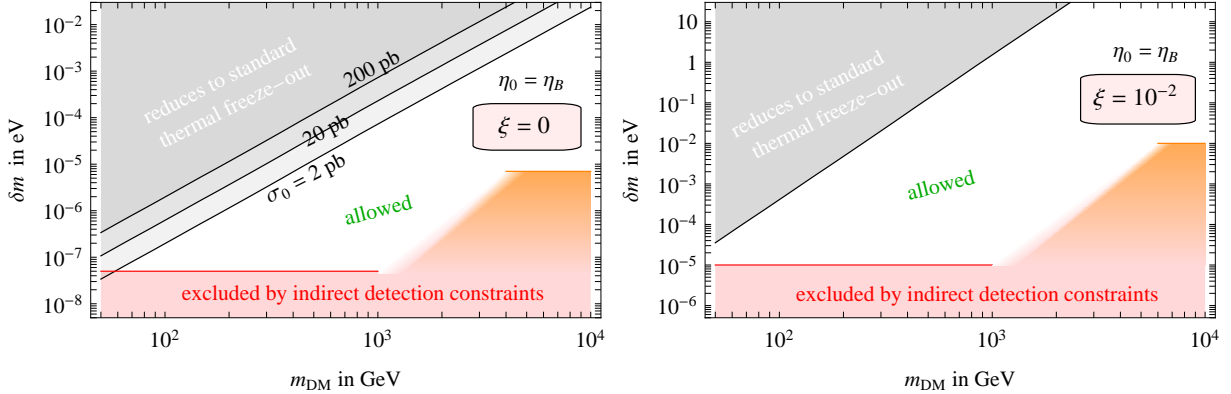


Figure 5: *Approximate illustration of the relevant parameter space in the scenarios we are considering, for the case without elastic scatterings (**left panel**) and for the case with scatterings (**right panel**). The upper left area shaded in grey corresponds to the region in which the evolution reduces to the standard freeze-out scenario. The white region refers to a regime in which oscillations recouple annihilations on cosmological scales and we always assume that a suitable value for the annihilation cross section is adopted for a given choice of m_{DM} and δm such that we reproduce the correct relic abundance. The lower area shaded in pink/orange is excluded by the constraints discussed in Sec. 5 (red is for FERMI and orange for H.E.S.S., see Fig. 6) either because it requires a too high cross section in ‘our’ regime, or because the value of δm is such that oscillations do not recouple annihilations on the cosmological scales, and we are back to a usual WIMP scenario. The fuzzy edge in the large m_{DM} portion indicates that it is not possible to individuate a single δm in the area where the H.E.S.S. constraints matter. We stress that these figures only illustrate the approximate areas of interest on the basis of eq. (36), while the results in all other plots in fig. 4 and 6 are determined by the full numerical solutions.*

value. In this case the annihilation rate is determined only by σ_0 , as usual. In other words, when this condition is satisfied we do not have to worry about the time dependence of the populations of the two species (and therefore of the annihilation rate) or about possible partial repopulations of one of the two species.

BBN. The period of the synthesis of nuclei in the primordial plasma (i.e. Big Bang Nucleosynthesis (BBN)) is the earliest test of standard cosmology, constraining the properties of the Universe starting from when it was a few seconds old, or equivalently at the MeV temperature scale. The good agreement of predicted abundances of the light elements with their measured values makes BBN a powerful cosmological probe: injections of particles and energy due to DM annihilation or decay, either during BBN, or at later times when those abundances are established, are constrained, as they would alter the observed abundances of primordial elements with respect to prediction (for a review see [67]).

More precisely, BBN can offer in principle two types of probes for the scenarios in which we are interested. If oscillations start well before BBN, DM annihilations could be happening at a low level during the BBN (without significantly changing Ω_{DM}) and the usual constraints on σ_0 during that era would apply (see e.g. [68]). However these constraints are typically weaker than the ones we will discuss below. A second, more attractive possibility arises if oscillations start *after* the end of BBN, i.e. if $t_{\text{osc}} > t_{\text{BBN}}$. In that case, as annihilations recouple, a large amount of energy is injected into the plasma. The set-up is similar to the one of late-decaying heavy DM progenitor states. Such decays

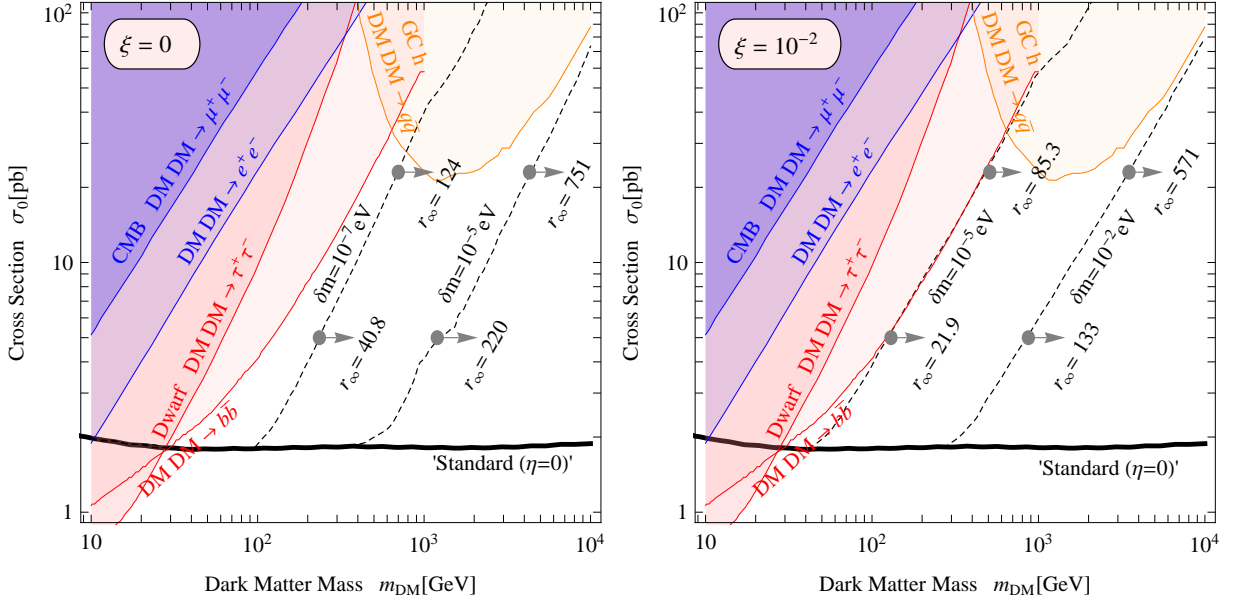


Figure 6: Summary plots of the parameter space, showing also the constraints. The dotted lines mark the contours along which a correct $\Omega_{\text{DM}} h^2$ can be obtained. **Left:** Oscillations and annihilations only ($\xi = 0$). **Right:** Including elastic scatterings ($\xi = 10^{-2}$). In both panels we assume an initial asymmetry $\eta_0 = \eta_B$ and we show two indicative values of the oscillation parameter δm . The solid black line at the bottom represents the standard case ($\eta = 0, \delta m = 0$). At some points on the contours, we provide the value of the ratio r defined in eq. (34). The shaded blue regions are excluded by CMB constraints, the shaded pink ones are disfavored by gamma ray observations with FERMI and the orange ones by observations with H.E.S.S. (see text). The white areas above the solid black line are allowed.

have been extensively studied and stringent constraints set, in the energy injection versus injection time plane. If the characteristic time t_{osc} is longer than 0.1 s, we would in fact be in a position to constrain the amount of energy stored in the dark sector before oscillations start, i.e. the initial value of DM asymmetry η_0 . However, once again, this possibility appears to be ruled out in the set-up in which we are interested, since $t_{\text{osc}} \lesssim 0.1$ sec on all the regions of the parameter space which are not already ruled out by the other constraints we discussed below.

Epoch of Reionization and CMB. Strong constraints are imposed on DM annihilations from considering the effect on the generation of the CMB anisotropies at the epoch of recombination (at redshift ~ 1100) and their subsequent evolution down to the epoch of reionization. The actual physical effect of energy injection around the recombination epoch is that it results in an increased amount of free electrons, which survive to lower redshifts and affect the CMB anisotropies [69]. Detailed constraints have been recently derived in [70], based on the WMAP (7-year) and Atacama Cosmology Telescope 2008 data. The constraints are somewhat sensitive to the dominant DM annihilation channel: annihilation modes for which a portion of the energy is carried away by neutrinos or stored in protons have a lesser impact on the CMB; on the contrary the annihilation mode which produces directly e^+e^- is the most effective one.

We reproduce in fig. 6 the constraints on our parameter space as obtained in [70], for

the two most stringent channels. It happens that the bounds run with the same slope in the $(m_{\text{DM}}, \sigma_0)$ plane as the lines of constant Ω_{DM} . One sees that, roughly, only the parameter space below $\delta m \geq 10^{-9}$ eV (10^{-7} eV) is allowed for the case of $\xi = 0$ ($\xi = 10^{-2}$), independently on the DM mass.

Present epoch γ -rays. For most of the DM annihilation modes, another relevant constraint is in fact imposed by the indirect DM searches in the present epoch. The DM constraints provided by the FERMI-LAT gamma ray data are particularly relevant as they are now cutting into the $\sigma_0 \sim 1$ pb value for low DM mass ($\lesssim 30$ GeV) and a variety of channels. In particular, dwarf satellite galaxies of the Milky Way are among the most promising targets for dark matter searches in gamma-rays because of their large dynamical mass to light ratio and small expected background from astrophysical sources. No dwarf galaxy has been detected in gamma rays so far and stringent upper limits are placed on DM annihilation by applying a joint likelihood analysis to 10 satellite galaxies with 2 years of FERMI-LAT data, taking into account the uncertainty in the dark matter distribution in the satellites [71]. The limits are particularly strong for hadronic annihilation channels, and somewhat weaker for leptonic channels as diffusion of leptons out of these systems is poorly constrained. On the other hand, strong limits on leptonic ($\mu^+\mu^-$) annihilation channels are set by, for example, the gamma-ray diffuse emission measurement at intermediate latitudes, which probes DM annihilation in our Milky Way halo. In particular, the most recent limits come from 2 years of the FERMI-LAT data in the $5^\circ \leq b \leq 15^\circ$, $-80^\circ \leq \ell \leq 80^\circ$ region [72], where b and ℓ are the galactic latitude and longitude.

Another relevant constraint in the large mass region is imposed by the observation of the Galactic Center halo with the H.E.S.S. telescope [73]. This refers to a $q\bar{q}$ annihilation channel and assumes that the DM distribution in the Galaxy follows a Navarro-Frenk-White or Einasto profile (notice that the constraint is lifted in case of a cored profile: the search is made by contrasting the source region closer to the GC with a background region further away, and, in case of a cored profile, both would yield the same DM flux).

We superimpose all these constraints on the plane in fig. 6. We see that they are somewhat stronger than the CMB ones considered above. We keep however the latter as they are less model dependent. More generally, we stress that all these constraints are valid under different (somewhat mutually exclusive) assumptions, such as e.g. the DM annihilation channel or the DM galactic profile. As a consequence, while we report all of them on the same plane for completeness, the precise regions of the parameter space which are actually excluded depend on the precise DM model.

Collider constraints. Finally, we also mention the constraints imposed by collider searches for dark matter [74]: in the framework of an effective field theory, the annihilation cross section of two DM particles into SM particles can be related to their production cross section in proton-antiproton collisions (Tevatron), proton-proton collisions (LHC) or e^+e^- ones (LEP), and therefore constrained by the searches at these respective machines. Current constraints are particularly relevant at low masses, and in some cases compete in strength with the bounds discussed above, while the LHC will soon extend the reach at larger masses. Contrary to the constraints discussed above, however, the collider ones ultimately rely on the assumption that DM couples via contact operators to the SM particles in the initial states of the collision process. E.g. DM annihilating into metastable new light states that then decay into SM particles cannot be constrained this way. We prefer therefore not to show them on the parameter space.

In the light of these bounds, many of the illustrative points presented in Fig. 3 are

excluded since they correspond to low masses, except for point C. As our final result, we focus therefore on the allowed region and show in the panels of Fig. 6, which are our final summary plots, the contour lines for $\Omega_{\text{DM}} h^2 = 0.11$. We also indicate, for some chosen points, the value of the ratio r defined in eq. (34).

6 Conclusions

In this work we have studied the impact of adding oscillations between DM and $\overline{\text{DM}}$ particles on the scenario of Asymmetric Dark Matter. Such oscillations arise naturally in aDM models, as we argued in Sec. 2, and should therefore be included. We found in particular that a typical WIMP with a mass at the EW scale ($\sim 100 \text{ GeV} - 1 \text{ TeV}$) presenting a primordial asymmetry of the same order as the baryon asymmetry naturally gets the correct relic abundance if the $\Delta(\text{DM}) = 2$ mass term is in the $\sim \text{meV}$ range. This turns out to be a natural value for fermionic DM arising from the higher dimensional operator $H^2 \text{DM}^2 / \Lambda$ where H is the Higgs field and $\Lambda \sim M_{\text{GUT}} - M_{\text{Pl}}$.

We have outlined the formalism (based on following the evolution of the density matrix of DM and $\overline{\text{DM}}$ populations) needed to treat the system of particles that oscillate coherently but at the same time suffer coherence-breaking elastic scatterings on the plasma and annihilations among themselves. Our formalism starts from a standard simplified form of the equation for the density matrix (eq. (11)) and makes use of a few simplifications (see Sec. 3 for a full discussion) but nevertheless is sufficient to illustrate the qualitative features that enter into play and that we want to stress. It would certainly be interesting to write a more rigorous set of equations derived from first principles. This is presently a very active field of research and still under development, in particular in the baryogenesis and leptogenesis community [76]. Those developments would be relevant for a more precise treatment of the problems that we are interested in here or for further complications of the picture (such as including CP violation in the game).

We have then applied such formalism to explore the phenomenologically available space, by varying the parameters of the dark matter mass m_{DM} , the annihilation cross section σ_0 , the primordial asymmetry in the DM sector η_0 and the mass difference δm which governs oscillations, for two discrete choices of the parameter ξ that sets the strength of the elastic scatterings between DM and the plasma. The quantitative results are displayed in fig. 4, which illustrates the exploration of the parameter space, and in fig. 6, which takes into account the constraints and focuses on the still allowed regions.

Our main result is readily summarized: we have shown that the parameter space at disposal becomes much wider and richer and in particular it is possible to have models of asymmetric DM with large m_{DM} (and large annihilation cross section) while still reproducing the right relic abundance $\Omega_{\text{DM}} h^2$ in the Universe. In other words, the mass and annihilation cross section of asymmetric WIMP dark matter are almost unconstrained by the relic density condition (for masses above $\sim 10 \text{ GeV}$ and for annihilation cross sections larger than the thermal one), as soon as we introduce oscillations. The main physical reason and the underlying mechanism are simple to understand: while in aDM the population of DM particles is frozen by the lack of targets, the oscillations re-symmetrize DM and $\overline{\text{DM}}$ particles, therefore allowing annihilations (if strong enough) to deplete them further until freeze-out; a smaller final number density accommodates a larger m_{DM} .

In this setup, therefore, $\Omega_{\text{DM}} h^2$ is no longer solely controlled by the primordial asymmetry

symmetric DM	$\Omega_{\text{DM}} \propto \sigma_0^{-1}$
asymmetric DM	<p style="text-align: center;">• <u>if $\xi = 0$ (negligible scattering):</u></p> $\Omega_{\text{DM}} \simeq \frac{m_{\text{DM}} s}{\rho_{\text{crit}}} \eta_0 \left[1 + 4806 \left(\frac{g_{*s,\infty}^4}{g_{*s,\infty}^3} \frac{\delta m^2}{\text{eV}^2} \left(\frac{\sigma_0}{\text{pb}} \right)^4 \left(\frac{\eta_0}{\eta_{\text{B}}} \right)^4 \right)^{1/5} \right]^{-1}$ $\Omega_{\text{DM}} \approx \frac{m_{\text{DM}} s}{\rho_{\text{crit}}} \begin{cases} \eta_0 & \text{if } \delta m \ll \delta m' \\ 2 \cdot 10^{-12} \eta_0^{1/5} \left(\frac{g_{*s,\infty}^3}{g_{*s,\infty}^4} \frac{\text{eV}^2 \text{ pb}^4}{\delta m^2 \sigma_0^4} \right)^{1/5} & \text{if } \delta m \gg \delta m' \end{cases}$ <p style="text-align: center;">with $\delta m' \approx 6.2 \cdot 10^{-10} \frac{g_{*s,\infty}^{3/2}}{g_{*s,\infty}^2} \left(\frac{\text{pb}}{\sigma_0} \right)^2 \left(\frac{\eta_{\text{B}}}{\eta_0} \right)^2 \text{ eV}$</p> <p style="text-align: center;">• <u>if $\xi \neq 0$ (scattering with primordial plasma):</u></p> $\Omega_{\text{DM}} \simeq \frac{m_{\text{DM}} s}{\rho_{\text{crit}}} \eta_0 \left[1 + 6.94 \frac{g_{*s,\infty}}{g_{*s,\infty}^{4/7}} \left(\frac{\delta m/\text{eV}}{\xi} \right)^{2/7} \frac{\sigma_0}{1 \text{ pb}} \frac{\eta_0}{\eta_{\text{B}}} \right]^{-1}$ $\Omega_{\text{DM}} \approx \frac{m_{\text{DM}} s}{\rho_{\text{crit}}} \begin{cases} \eta_0 & \text{if } \delta m \ll \delta m'' \\ 1.4 \cdot 10^{-11} \xi \frac{g_{*s,\infty}^{4/7}}{g_{*s,\infty}} \frac{\text{pb}}{\sigma_0} \left(\frac{\text{eV}}{\delta m} \right)^{2/7} & \text{if } \delta m \gg \delta m'' \end{cases}$ <p style="text-align: center;">with $\delta m'' \approx 10^{-3} \xi \left(\frac{g_{*s,\infty}}{g_{*s,\infty}^{4/7}} \frac{\sigma_0}{1 \text{ pb}} \frac{\eta_0}{\eta_{\text{B}}} \right)^{-7/2} \text{ eV}$</p>

Table 1: Scaling of the WIMP relic abundance with the DM parameters m_{DM} , δm , σ_0 and the primordial asymmetry η_0 . The scattering of DM with the plasma is parametrized by $\xi = G_{\text{DM}}/G_{\text{F}}$ where G_{DM} is the analog of the Fermi constant for the coupling of DM to matter. The formulæ follow eq. (30)–(33) and are valid for σ_0 not too large (see text in Sec. 4 for details).

η_0 , like in the aDM case, and no longer solely controlled by the annihilation cross section $\langle \sigma v \rangle$, like in the thermal freeze-out case, but instead a smooth bridge is provided between the two. The scaling of Ω_{DM} with parameters is given in eq. (30)–(33) and it is also summarized explicitly in Table 1. These scenarios can thus preserve the attractive feature of aDM, that relates the DM primordial asymmetry and the baryon asymmetry in the first place, but at the same time preserve also the appeal of weak-scale DM mass (and possibly cross-sections). Note that vanilla aDM models with $m_{\text{DM}} \sim$ a few GeV are ruled out unless δm is effectively zero.

As a last remark, we note that the dark sector may turn out to be more complicated than studied here. For instance, the WIMP sector may contain different flavours that could mix or there could be mixing between the WIMP and standard neutrinos. These effects have been extensively discussed in the case of sterile neutrino dark matter but not so in the case of WIMP dark matter, apart from the case of sneutrinos, e.g [78]. A recent interest for

these possibilities has arisen [37, 40, 77], although the consequences for the relic abundance of WIMPs have not yet been studied in detail (see however the recent Ref. [79]). A new future interesting direction of investigation is therefore opening.

Note. While this work was being completed, Ref. [80], whose scope is similar to ours, appeared. Contrasting our procedure with theirs, we note that they used a simplified Boltzmann equation that treats the oscillations with a constant rate and in a way that does not include decoherence effects due to annihilations. They also do not include elastic scatterings. A comparison between the formalisms can be readily done using the Boltzmann-like equations (24) derived from the matrix formalism: in our full form, the differential equation for the sum $\Sigma = Y^+ + Y^-$ is affected by the evolution of the difference $\Delta = Y^+ - Y^-$ as well as the evolution of the off-diagonal elements of the density matrix Ξ . In Ref. [80], $\Xi'(x) = 0$ and the equation for Δ does not depend on annihilations nor scatterings, namely $\Delta'(x)/\Delta = -2\delta m/(xH(x))$, in contrast with what Eq. (24) indicates (see the discussion at page 10). This leads to a different damping factor in the evolution of $\Sigma(x)$. The simplified approach of [80] can lead to a different or even very different time evolution with respect to the full approach that we pursue. Quantitatively, the discrepancy between the simplified and the full approaches varies depending on the choices of parameters. For a significant range of parameter space, both approaches lead to the same relic abundance (up to $\mathcal{O}(1)$ deviations), as we illustrate in an example in Fig. 7 on the left. For other choices, however, the two approaches produce a final relic abundance that differs by more than one order of magnitude (see e.g. the right panel in Fig. 7). To recap, our formalism has the advantage of allowing to describe oscillations consistently as well as to take into account elastic scatterings. Finally, we have provided a full exploration of the parameter space and we are interested in identifying the choices of parameters for which the correct Ω_{DM} is obtained, while [80] focusses on two specific values of the DM mass and does not require that the correct DM relic abundance is reproduced.

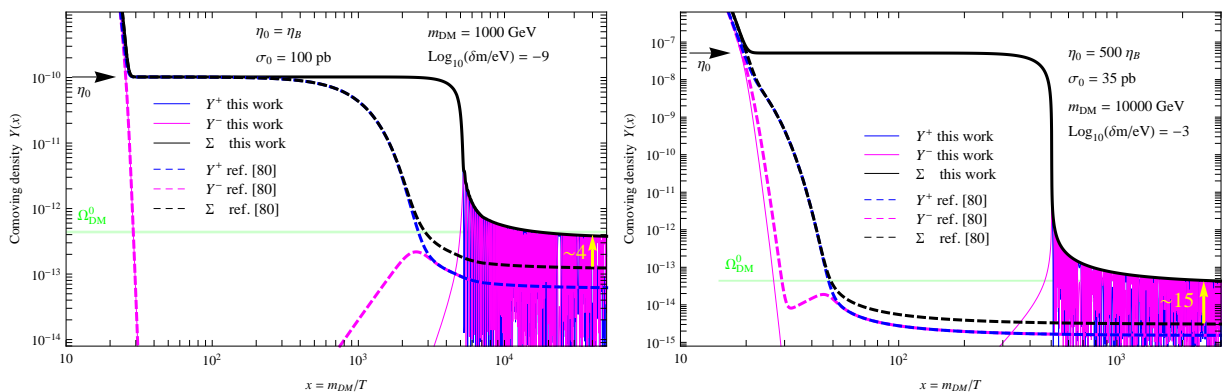


Figure 7: Comparison with the results of [80], for two specific choices of parameters (indicated).

Acknowledgements We thank Zurab Berezhiani, Adam Falkowski, Alex Friedland, Thomas Konstandin, Kimmo Kainulainen, Thomas Schwetz-Mangold, Thomas Hambye and Pasquale Serpico for useful discussions. This work is supported by the ERC starting Grant Cosmo@LHC, by the French national research agency ANR under contract ANR 2010

BLANC 041301 and by the EU ITN network UNILHC. Part of it was completed during the CERN TH-Institute *DMUH'11* (18-29 July 2011). We also acknowledge support from the Institut de Physique of CNRS within the ‘*PEPS 2010 Projets - Physique Théorique et ses Interfaces*’.

References

- [1] See e.g. E. Komatsu *et al.* [WMAP Collaboration], *Astrophys. J. Suppl.* **192** (2011) 18 [arXiv:1001.4538v3 [astro-ph.CO]].
- [2] See e.g. G. Gelmini, P. Gondolo, In *Bertone, G. (ed.): Particle Dark Matter*, 121-141 [arXiv:1009.3690 [astro-ph.CO]]; B. S. Acharya, G. Kane, S. Watson and P. Kumar, *Phys. Rev. D* **80** (2009) 083529 [arXiv:0908.2430 [astro-ph.CO]]; D. J. H. Chung, E. W. Kolb, A. Riotto, *Phys. Rev. Lett.* **81** (1998) 4048-4051 [hep-ph/9805473].
- [3] A. Boyarsky, O. Ruchayskiy, M. Shaposhnikov, *Ann. Rev. Nucl. Part. Sci.* **59** (2009) 191-214 [arXiv:0901.0011 [hep-ph]].
- [4] L. J. Hall, K. Jedamzik, J. March-Russell, S. M. West, *JHEP* **1003**, 080 (2010) [arXiv:0911.1120 [hep-ph]].
- [5] S. Nussinov, *Phys. Lett. B* **165** (1985) 55.
- [6] S. M. Barr, R. S. Chivukula and E. Farhi, *Phys. Lett. B* **241** (1990) 387.
- [7] S. M. Barr, *Phys. Rev. D* **44** (1991) 3062-3066.
- [8] D. B. Kaplan, *Phys. Rev. Lett.* **68** (1992) 741.
- [9] S. B. Gudnason, C. Kouvaris, F. Sannino, *Phys. Rev. D* **73** (2006) 115003 [hep-ph/0603014].
S. B. Gudnason, C. Kouvaris, F. Sannino, *Phys. Rev. D* **74** (2006) 095008 [hep-ph/0608055].
- [10] H. M. Hodges, *Phys. Rev. D* **47** (1993) 456-459.
- [11] R. Foot, R. R. Volkas, *Phys. Rev. D* **52** (1995) 6595-6606 [hep-ph/9505359].
- [12] Z. G. Berezhiani, R. N. Mohapatra, *Phys. Rev. D* **52** (1995) 6607-6611 [hep-ph/9505385].
- [13] Z. G. Berezhiani, A. D. Dolgov, R. N. Mohapatra, *Phys. Lett. B* **375** (1996) 26-36 [hep-ph/9511221].
- [14] L. Bento, Z. Berezhiani, [hep-ph/0111116].
- [15] Z. Berezhiani, “Through the looking-glass: Alice’s adventures in mirror world,” In *Shifman, M. (ed.) et al.: From fields to strings, vol. 3*, 2147-2195 [hep-ph/0508233].
- [16] R. Foot, R. R. Volkas, *Phys. Rev. D* **68** (2003) 021304. [hep-ph/0304261]. R. Foot, R. R. Volkas, *Phys. Rev. D* **69** (2004) 123510. [hep-ph/0402267].
- [17] G. R. Farrar, G. Zaharijas, *Phys. Rev. Lett.* **96** (2006) 041302 [hep-ph/0510079].
- [18] D. Hooper, J. March-Russell, S. M. West, *Phys. Lett. B* **605** (2005) 228-236 [hep-ph/0410114].
- [19] R. Kitano, I. Low, *Phys. Rev. D* **71** (2005) 023510 [hep-ph/0411133].
- [20] K. Agashe, G. Servant, *JCAP* **0502** (2005) 002 [hep-ph/0411254].
- [21] N. Cosme, L. Lopez Honorez, M. H. G. Tytgat, *Phys. Rev. D* **72** (2005) 043505 [hep-ph/0506320].
- [22] K. Belotsky, D. Fargion, M. Khlopov, R. V. Konoplich, *Phys. Atom. Nucl.* **71** (2008) 147-161. [hep-ph/0411093]. M. Y. Khlopov, *Pisma Zh. Eksp. Teor. Fiz.* **83** (2006) 3-6. [astro-ph/0511796].
- [23] D. E. Kaplan, M. A. Luty and K. M. Zurek, *Phys. Rev. D* **79** (2009) 115016 [arXiv:0901.4117 [hep-ph]].
- [24] T. Cohen and K. M. Zurek, *Phys. Rev. Lett.* **104** (2010) 101301 [arXiv:0909.2035 [hep-ph]].
- [25] Y. Cai, M. A. Luty, D. E. Kaplan, [arXiv:0909.5499 [hep-ph]].
- [26] H. An, S.-L. Chen, R. Mohapatra, Y. Zhang, *JHEP* **1003** (2010) 124 [arXiv:0911.4463 [hep-ph]].
- [27] J. Shelton and K. M. Zurek, *Phys. Rev. D* **82** (2010) 123512 [arXiv:1008.1997 [hep-ph]].
- [28] M. R. Buckley, L. Randall, *JHEP* **1109** (2011) 009. [arXiv:1009.0270 [hep-ph]].
- [29] H. Davoudiasl, D. E. Morrissey, K. Sigurdson and S. Tulin, *Phys. Rev. Lett.* **105** (2010) 211304 [arXiv:1008.2399 [hep-ph]].
- [30] N. Haba, S. Matsumoto, *Prog. Theor. Phys.* **125** (2011) 1311-1316. [arXiv:1008.2487 [hep-ph]].
- [31] E. J. Chun, *Phys. Rev. D* **83** (2011) 053004 [arXiv:1009.0983 [hep-ph]].

- [32] P.-H. Gu, M. Lindner, U. Sarkar, X. Zhang, Phys. Rev. **D83** (2011) 055008. [arXiv:1009.2690 [hep-ph]].
- [33] M. Blennow, B. Dasgupta, E. Fernandez-Martinez, N. Rius, JHEP **1103** (2011) 014. [arXiv:1009.3159 [hep-ph]].
- [34] J. McDonald, arXiv:1009.3227 [hep-ph].
- [35] R. Allahverdi, B. Dutta, K. Sinha, Phys. Rev. **D83** (2011) 083502. [arXiv:1011.1286 [hep-ph]].
- [36] B. Dutta, J. Kumar, Phys. Lett. **B699** (2011) 364-367. [arXiv:1012.1341 [hep-ph]].
- [37] A. Falkowski, J. T. Ruderman, T. Volansky, JHEP **1105** (2011) 106. [arXiv:1101.4936 [hep-ph]].
- [38] C. Cheung, K. M. Zurek, Phys. Rev. **D84** (2011) 035007. [arXiv:1105.4612 [hep-ph]].
- [39] E. Del Nobile, C. Kouvaris, F. Sannino, Phys. Rev. **D84** (2011) 027301. [arXiv:1105.5431 [hep-ph]].
- [40] Y. Cui, L. Randall, B. Shuve, [arXiv:1106.4834 [hep-ph]].
- [41] J. March-Russell, M. McCullough, [arXiv:1106.4319 [hep-ph]].
- [42] M. T. Frandsen, S. Sarkar, K. Schmidt-Hoberg, Phys. Rev. **D84** (2011) 051703. [arXiv:1103.4350 [hep-ph]].
- [43] M. R. Buckley, Phys. Rev. **D84** (2011) 043510. [arXiv:1104.1429 [hep-ph]].
- [44] H. Davoudiasl, D. E. Morrissey, K. Sigurdson, S. Tulin, [arXiv:1106.4320 [hep-ph]].
- [45] M. L. Graesser, I. M. Shoemaker, L. Vecchi, [arXiv:1107.2666 [hep-ph]].
- [46] C. Arina, N. Sahu, [arXiv:1108.3967 [hep-ph]].
- [47] J. McDonald, [arXiv:1108.4653 [hep-ph]].
- [48] S. M. Barr, [arXiv:1109.2562 [hep-ph]].
- [49] A. L. Fitzpatrick, D. Hooper, K. M. Zurek, Phys. Rev. **D81** (2010) 115005 [arXiv:1003.0014 [hep-ph]]. H. An, S. -L. Chen, R. N. Mohapatra, S. Nussinov, Y. Zhang, Phys. Rev. **D82** (2010) 023533 [arXiv:1004.3296 [hep-ph]]. N. Fornengo, P. Panci, M. Regis, [arXiv:1108.4661 [hep-ph]].
- [50] M. L. Graesser, I. M. Shoemaker and L. Vecchi, arXiv:1103.2771 [hep-ph].
- [51] H. Imminiyaz, M. Drees and X. Chen, arXiv:1104.5548 [hep-ph].
- [52] M. T. Frandsen and S. Sarkar, Phys. Rev. Lett. **105** (2010) 011301 [arXiv:1003.4505 [hep-ph]]. B. Feldstein, A. L. Fitzpatrick, JCAP **1009**, 005 (2010). [arXiv:1003.5662 [hep-ph]]. D. T. Cumberbatch, J. A. Guzik, J. Silk, L. S. Watson, S. M. West, Phys. Rev. **D82** (2010) 103503 [arXiv:1005.5102 [astro-ph.SR]]. M. Taoso, F. Iocco, G. Meynet, G. Bertone and P. Eggenberger, Phys. Rev. D **82** (2010) 083509 [arXiv:1005.5711 [astro-ph.CO]]. C. Kouvaris, P. Tinyakov, Phys. Rev. **D83** (2011) 083512 [arXiv:1012.2039 [astro-ph.HE]]. S. D. McDermott, H. -B. Yu, K. M. Zurek, [arXiv:1103.5472 [hep-ph]]. C. Kouvaris and P. Tinyakov, arXiv:1104.0382 [astro-ph.CO].
- [53] S. M. Bilenky and S. T. Petcov, Rev. Mod. Phys. **59** (1987) 671 [Erratum-ibid. **61** (1989) 169] [Erratum-ibid. **60** (1988) 575].
- [54] M. Hirsch, H. V. Klapdor-Kleingrothaus, S. G. Kovalenko, Phys. Lett. **B398** (1997) 311-314. [hep-ph/9701253].
- [55] Y. Grossman, H. E. Haber, Phys. Rev. Lett. **78** (1997) 3438-3441. [hep-ph/9702421].
- [56] L. J. Hall, T. Moroi, H. Murayama, Phys. Lett. **B424** (1998) 305-312. [hep-ph/9712515].
- [57] K. Choi, K. Hwang, W. Y. Song, Phys. Rev. Lett. **88** (2002) 141801. [hep-ph/0108028].
- [58] D. Tucker-Smith, N. Weiner, Phys. Rev. **D64** (2001) 043502. [hep-ph/0101138].
- [59] Y. Cui, D. E. Morrissey, D. Poland, L. Randall, JHEP **0905** (2009) 076. [arXiv:0901.0557 [hep-ph]].
- [60] M. Lindner, D. Schmidt, T. Schwetz, [arXiv:1105.4626 [hep-ph]]. See also: E. J. Chun, Phys. Lett. B **525** (2002) 114 [arXiv:hep-ph/0105157].
- [61] E. Ma, Phys. Rev. **D73** (2006) 077301. [hep-ph/0601225].
- [62] The formalism for the propagation of interacting and oscillating neutrinos has been fully presented in G. Raffelt, G. Sigl, L. Stodolsky, Phys. Rev. Lett. **70** (1993) 2363-2366 [hep-ph/9209276], G. Sigl, G. Raffelt, Nucl. Phys. **B406** (1993) 423-451, although it had been pioneeringly introduced in A. D. Dolgov, Sov. J. Nucl. Phys. **33** (1981) 700-706 (A. D. Dolgov, Yad. Fiz. **33**, 1309 (1981) and R. Barbieri, A. Dolgov, Nucl. Phys. **B349** (1991) 743-753. A collection of results is found in A. D. Dolgov, Phys. Rept. **370** (2002) 333-535 [hep-ph/0202122].

- [63] See R. J. Scherrer, M. S. Turner, Phys. Rev. **D34** (1986) 3263, which is the *Erratum* of the Appendix of R. J. Scherrer, M. S. Turner, Phys. Rev. **D33** (1986) 1585.
- [64] M. C. Gonzalez-Garcia, Y. Nir, Rev. Mod. Phys. **75** (2003) 345-402 [[hep-ph/0202058](#)]. A. Strumia, F. Vissani, [[hep-ph/0606054](#)].
- [65] K. Abazajian, G. M. Fuller, M. Patel, Phys. Rev. **D64**, 023501 (2001). [[astro-ph/0101524](#)].
- [66] S. Dodelson, L. M. Widrow, Phys. Rev. Lett. **72**, 17-20 (1994). [[hep-ph/9303287](#)].
- [67] F. Iocco, G. Mangano, G. Miele, O. Pisanti, P. D. Serpico, Phys. Rept. **472**, 1-76 (2009) [[arXiv:0809.0631](#) [[astro-ph](#)]].
- [68] J. Hisano, M. Kawasaki, K. Kohri, T. Moroi, K. Nakayama, T. Sekiguchi, Phys. Rev. **D83**, 123511 (2011) [[arXiv:1102.4658](#) [[hep-ph](#)]].
- [69] S. Galli, F. Iocco, G. Bertone, A. Melchiorri, Phys. Rev. **D80** (2009) 023505 [[arXiv:0905.0003](#) [[astro-ph.CO](#)]].
T. R. Slatyer, N. Padmanabhan, D. P. Finkbeiner, Phys. Rev. **D80** (2009) 043526 [[arXiv:0906.1197](#) [[astro-ph.CO](#)]].
G. Huetsi, A. Hektor, M. Raidal, Astron. Astrophys. **505** (2009) 999-1005 [[arXiv:0906.4550](#) [[astro-ph.CO](#)]].
M. Cirelli, F. Iocco, P. Panci, JCAP **0910** (2009) 009 [[arXiv:0907.0719](#) [[astro-ph.CO](#)]].
- [70] G. Hutsi, J. Chluba, A. Hektor, M. Raidal [[arXiv:1103.2766](#) [[astro-ph.CO](#)]].
S. Galli, F. Iocco, G. Bertone, A. Melchiorri [[arXiv:1106.1528](#) [[astro-ph.CO](#)]].
- [71] The FERMI-LAT collaboration, [[arXiv:1108.3546](#) [[astro-ph.HE](#)]]. See also: talk by Maja L. Garde at the [FERMI Symposium 2011](#).
- [72] M. Cirelli, P. Panci, P. D. Serpico, Nucl. Phys. **B840**, 284-303 (2010) [[arXiv:0912.0663](#) [[astro-ph.CO](#)]].
M. Papucci, A. Strumia, JCAP **1003**, 014 (2010) [[arXiv:0912.0742](#) [[hep-ph](#)]].
- G. Zaharijas *et al.* [for the Fermi-LAT Collaboration], [[arXiv:1012.0588](#) [[astro-ph.HE](#)]] and talk by G. Zaharijas at the [FERMI Symposium 2011](#).
- [73] A. Abramowski *et al.* [H.E.S.S. Collaboration], Phys. Rev. Lett. **106** (2011) 161301. [[arXiv:1103.3266](#) [[astro-ph.HE](#)]].
- [74] J. Goodman, M. Ibe, A. Rajaraman, W. Shepherd, T. M. P. Tait, H.-B. Yu, Phys. Lett. **B695** (2011) 185-188 [[arXiv:1005.1286](#) [[hep-ph](#)]]. Y. Bai, P. J. Fox, R. Harnik, JHEP **1012** (2010) 048, [[arXiv:1005.3797](#) [[hep-ph](#)]]. J. Goodman, M. Ibe, A. Rajaraman, W. Shepherd, T. M. P. Tait, H.-B. Yu, Phys. Rev. **D82** (2010) 116010. [[arXiv:1008.1783](#) [[hep-ph](#)]]. P. J. Fox, R. Harnik, J. Kopp, Y. Tsai, [[arXiv:1103.0240](#) [[hep-ph](#)]].
- [75] A. D. Dolgov, S. H. Hansen, S. Pastor, D. V. Semikoz, Astropart. Phys. **14** (2000) 79-90. [[arXiv:hep-ph/9910444](#) [[hep-ph](#)]].
- [76] E.g. A. Anisimov, W. Buchmuller, M. Drewes, S. Mendizabal, Annals Phys. **326** (2011) 1998-2038. [[arXiv:1012.5821](#) [[hep-ph](#)]]. C. Fidler, M. Herranen, K. Kainulainen and P. M. Rakhila, [[arXiv:1108.2309](#) [[hep-ph](#)]]. M. Beneke, B. Garbrecht, C. Fidler, M. Herranen and P. Schwaller, Nucl. Phys. B **843** (2011) 177 [[arXiv:1007.4783](#) [[hep-ph](#)]]. J. S. Gagnon and M. Shaposhnikov, Phys. Rev. D **83** (2011) 065021 [[arXiv:1012.1126](#) [[hep-ph](#)]]. T. Konstandin, T. Prokopec, M. G. Schmidt, M. Seco, Nucl. Phys. **B738** (2006) 1-22. [[hep-ph/0505103](#)]. V. Cirigliano, C. Lee, M. J. Ramsey-Musolf, S. Tulin, Phys. Rev. **D81** (2010) 103503. [[arXiv:0912.3523](#) [[hep-ph](#)]].
- [77] P. Agrawal, S. Blanchet, Z. Chacko, C. Kilic, [[arXiv:1109.3516](#) [[hep-ph](#)]].
- [78] J. March-Russell, C. McCabe, M. McCullough, JHEP **1003** (2010) 108. [[arXiv:0911.4489](#) [[hep-ph](#)]].
- [79] H. Baer, A. Lessa, W. Sreethawong, [[arXiv:1110.2491](#) [[hep-ph](#)]].
- [80] M. R. Buckley, S. Profumo, [[arXiv:1109.2164v1](#) [[hep-ph](#)]].